Research on Mechanisms of Enhanced Oil Recovery Using Nano-Solution

ナノ粒子流体を使用した原油増進回収のメカニズムに関する研究

March 2022

Tito WIJAYANTO
ウィジャヤント　ティト

Research on Mechanisms of Enhanced Oil Recovery Using Nano-Solution

ナノ粒子流体を使用した原油増進回収のメカニズムに関する研究

March 2022

Waseda University Graduate School of Creative Science and Engineering

Department of Earth Sciences, Resources and Environmental Engineering,
Research on Petroleum Engineering

Tito WIJAYANTO
ウィジャヤント　ティト

March 2022

فَبِأَيِّ آلَاءِ رَبِّكُمَا تُكَذِّبَانِ.

Fa bi‘ayyi ālā‘i rabbikumā tukażżibān

-Then which of the favours of your Lord (Allah) will you deny-

This thesis is dedicated to my beloved wife and wonderful son,
Evi Amalia and Rasya Alvaro Wijayanto

Also, both of my parents, mother-in-law
brother and sister, and sister-in-laws

[this page was intentionally left blank]

"***Fossil fuels will remain the dominant source of energy powering the world economy. The demand for oil will continue to grow over the next 20 years, largely stemming from the strong growth in developing economies.***"

– Spencer Dale, *BP Chief Economist*, 2016 –

"***Several times in the past we have thought that we were running out of oil whereas actually, we were only running out of ideas.***"

– Parke A. Dickey, *Geologist*, 1958 –

[this page was intentionally left blank]

Summary

Worldwide energy consumption has grown significantly spurred by sustainable economic growth and increasing demand in developing countries. Fossil fuel, particularly oil, is still the primary energy source for many developing countries, especially Indonesia. Indonesian energy consumption is mainly driven by power generation, industrial demand, and increasing transport fuel consumption. To offset and provide a viable solution to this increase in energy demand, the government encourages operators to exercise brownfields recovery through enhanced oil recovery methodologies. New technological approaches are needed in order to be able to gain more oil from these mature oil fields, including nanotechnology, which is thought to help achieve this objective. The nanotechnologies have the capability to change the way that petroleum is explored and produced, and are tackled in both the upstream and downstream industries.

Meanwhile, the concept of the recovery mechanisms by nanoparticle injection remains unclear. In this thesis, laboratory experiments were carried out to obtain a fundamental concept of how nanoparticles displace the remaining oil in porous media and unlock nanoparticle potential as novel enhanced oil recovery agents.

Nanofluids are a novel class engineered liquid containing a two-phase structure (solid and liquid) and crucial to the new interdisciplinary area where nano-science, nanotechnology, and thermodynamic engineering come together. Nanofluids are nanoparticles dispersed in a base liquid. Hence, the stability of nanofluids is of paramount importance. Designing the desired stability of nanofluids over time and across temperatures is a considerable challenge. Most of the previous work has studied the effects of the nanoparticles from the standpoint of wettability and interfacial tension. In those studies, however, the nanoparticle suspensions were usually composed of bare nanoparticles and surfactants or stabilizers to prevent agglomeration, which could have affected measurements and made it ambiguous which components in the nanoparticle suspensions had played a role.

The ultimate objective of this thesis research is to substantiate the applicability and evaluate the performance of nanoparticles as one of the emerging technology in the enhanced oil recovery method at the laboratory scale before field deployment. In contrast, the specific objectives are described from a reservoir engineering point of view.

The research was conducted through designed laboratory experiments, such as wettability alteration measurements, interfacial tension measurements, and dis-

placement tests, and several parameters were studied. There are two series of laboratory experiments utilizing different types of nanoparticles. The first experiment used powder-shaped nanoparticles, and the second experiment used commercial nanofluids. These experiments were performed without using a stabilizer agent in order to avoid ambiguity and minimize costs.

The fumed synthesized hydrophilic aluminosilicate nanoparticles and a cationic-acidic Snowtex® ST-AK nanofluids were utilized in the first and second experiments, respectively, as the main nano-materials. The synthesis of the nanoparticles was not discussed and is beyond the scope of this research. As the research media, paraffinic crude oil and formation water were sampled from the Langgak field in Indonesia, and synthetic oil and synthetic brine were used for the first experiment and second experiment, respectively.

The following parts provide a brief explanation of every chapter of the thesis. Chapter 1-Introduction provides a brief background and motivation for this thesis. Chapter 2-Theoretical Background describes the theoretical background and fundamentals of nanoparticles, including relevant aspects and parameters to be investigated. Chapter 3-Aluminosilicate Nanoparticles for EOR Agent contains a description of the materials and their characterization, the methods and procedure for all experiments involved in fluid behavior, fluid-fluid, and fluid-rock interactions to the presence of nanoparticles. The laboratory experiments, including stability investigation, wettability determination using the Amott-Harvey methods, IFT measurement, and the displacement tests, are examined. This chapter reveals that the aluminosilicate nanoparticles solution with an optimum concentration was effective to make wettability of a reservoir more water-wet, which lead to the recovery of oil remained in water flooding. Chapter 4-Snowtex® ST-AK Nanofluids as an EOR Agent provides the procedures of the experiments, which include IFT measurement, wettability alteration measurement using contact angle determination, and the core flooding tests. This chapter presents that the driving mechanisms for enhancing oil recovery by this commercial nano-fluid was suspected to be the adsorption of nanoparticles resulting in the wettability alteration and the structural disjoining pressure. Chapter 5-Numerical Simulation of Nano-Solution Enhanced Oil Recovery provides information about numerical simulation with mathematical equations and formulas to reproduce the oil displacement experiments described in Chapter 3. Chapter 6-Conclusions and Recommendations summarize the main findings of this research and recommendations for further research.

Preface

The work entitled," Research on Mechanisms of Enhanced Oil Recovery using Nano-Solution" was intentionally written to fulfill the requirement of the degree, Doctor of Engineering, at Waseda University. Formulation of this thesis research work started back in April 2016 and the thesis writing finally can be concluded by February 2022. The research process was quite challenging, complicated, yet rewarding. The work on this thesis somehow took longer than I had predicted, yet the this challenging work turned out to be very fulfilling. I have not performed work in a University laboratory since my Bachelor Degree years and it took some time to get acclimated to the nuances of laboratory work again. I have experienced teething period to get used with laboratory, but it paid off. Today, without any doubt, I am more knowledgeable in regards to the field of nanoparticles and their role and uses in enhanced oil recovery.

I gained quite a fair amount of knowledge from Luky Hendraningrat, Ph.D. for preparing the question marks for this research prior to discussing with my supervisor, Professor Masanori Kurihara. From my supervisor, I have gained insight into the knowledge, experiences, and the how to methods in achieving my research objectives. I gained knwoledge from my laboratory partner, Utomo Pratama Iskandar, mainly how to commence and adapt the materials and equipment and compose numerical simulations for different research purposes. Also from Shintaro Sugiyama for doing me a favor to construct numerical simulation of nano-solution EOR. Several parts of this research were previously accepted in different peer-reviewed academic journals. The material in Chapters 3 and 4 of this thesis can be found in the following journals:

(1) Wijayanto, T., Kurihara, M., Kurniawan, T. and Muraza, O., 2019. Experimental investigation of aluminosilicate nanoparticles for enhanced recovery of waxy crude oil. *Energy & Fuels*, 33(7), pp.6076-6082.

(2) Wijayanto, T., Iskandar, U. P., Kurihara, M., Muraza, O., & Marhaendrajana, T. (2021). Application of functionalized cationic-acidic silica-alumina-based nanofluids for enhanced oil recovery. *Journal of the Japanese Association for Petroleum Technology*, 86(3), 194-204.

In addition, this lengthy work would be definitely impossible without the teamwork and cooperation of those at Waseda University and the Waseda University and Institute Technology of Bandung. Their amount of consistent hard work and dedication is truly commendable. Therefore, this knowledge becomes

extraordinary and most valuable journeys. I do hope that you will also experience the same feeling, mutual passion and enthusiasm as I did by reading my work.

Tokyo, March 2022
Tito Wijayanto

Acknowledgements

My profound gratitude goes to Allah the Almighty, the omnipotent and omniscient. All praise and glory are to Allah alone for giving me the wisdom, knowledge, health, time, resources, and opportunity to study on such an important and a hot issue these days. Peace and blessing of Allah be upon to Muhammad s.a.w, our noble Prophet, and his family, also his companions who follow his right path until the day of resurrection.

This book marks the end of my long and arduous Ph.D. journey. I am very grateful to the many people and organizations that contributed to the development of this research. Firstly, I am thankful to the respected many professor and administrative staff of the Graduate School of Creative Science and Engineering, Faculty of Science and Engineering at Waseda University. I would like to express my greatest appreciation to my esteemed my supervisor, Professor Masanori Kurihara, who was abundantly helpful and offered many an invaluable assistance, support, guidance, and advice during my Ph.D. research effort as well as for the practical guidance during preparation of the academic papers and this thesis, and also for the needed administrative work. Secondly, I would like to express my extreme gratitude to Professor Kenji Furui, Professor Takemi Ueda, and Hisanao Ouchi, Ph.D., whom all are the members of my Ph.D. committee. Thirdly, I am grateful to Luky Hendraningrat, Ph.D., and Dr. Oki Muraza, for their expert guidance, discussions, as well as their knowledge base in preparation of the research and peer-reviewed academic journals. I am also thankful to Ms. Kazu Koshigoe, Ms. Keiko Tanimoto, Ms. Kinuko Yanagi, Ms. Nao Yumizuka, Ms. Miyuki Ito and Ms. Asako Yamaoka for their kind help and cooperation at all times while I was conducting my studies and research. Also to my fellow laboratory members, Shintaro Sugiyama, Kyohei Inoue, Kenta Takahashi, Kotaro Takahashi, Masafumi Fukuhara, Kenta Sekine and Yasuhiro Kaneshima.

Foremost, I wish to express love and gratitude to my loving wife, Evi Amalia, and my wonderful son, Rasya Alvaro Wijayanto, for keeping my days beautiful, for their understanding, patience, and love through out the duration of my long and arduous studies to achieve my goal as a Doctor of Engineering. I do hope that this thesis report is a small compensation for their love, patience, and support. I would like to dedicate, my accomplished work, to the extraordinary people in my life, my parents, Surono Wongsowinoto and Yati Suprijati, especially for their love, caring, and dedication while raising me, seeing me achieve my goals, and not forgetting my sister, Yulia Suryanti, as well as my brother, Arie Wibowo, and to many family members for their unlimited support and encour-

agement. I also am grateful to all of my friends who also studied at Waseda, the 'mimisan' Genk -Mbak Anisah Alfada, Astri a.k.a Aci, Olfi a.k.a Sistaofi, Jati, Resna and Asep,- masbro Arief, masbro Sukarman, Elkana, Chrisenda, Vaya, and all members of PPI Waseda. Also to my colleague and laboratory partner, Utomo Pratama Iskandar, who proofread my works and participated in the unforgettable adventure with many bitter and sweet moments. A special thanks to my late departed soul mate Himawan Sutanto, may his soul rest in peace, and not forgetting Dr. Junita Trivianty Musu, who encouraged me to pursue a Ph.D. degree. Last but not least, to Mr. John van der Waal for proofreading all of my works.

I am grateful to Bapak Ikin Faisal, the Director of PT. SPR Langgak, Indonesia, and Satoru Murakami San from Nissan Chemical Corporation, Ltd, Japan, for providing the material support, and to the Institute Technology of Bandung, Indonesia for providing the laboratory apparatus for this research. I want to end this acknowledgment by thanking the Ministry of Energy and Mineral Resources Republic of Indonesia for providing me the needed scholarship to pursue this Ph.D. degree. Also, the people who supported me from the beginning to the end, Bapak Bambang Widarsono, Bapak Daru Siswanto, Bapak Abdul Haris, Bapak Usman Pasarai, Bapak Yuli Wahono, Bapak Maompang Harahap, Bapak Oktoaji Kharissuhud, Bapak Sri Sabdo Bawono, Bapak Yond Rizal, Ibu Nur Widyasari, and Ibu Upik Jamil. And not to forget, also, my supervisors and colleagues from Lemigas, Bapak Fadjril Rusita and Bapak Hendy Marendra, Zainal Abidin, Akhnis Dawafi, Irsyadul Hidayat, Dimas Ragil, Hestuti Eni and all of those whom I cannot mention one by one. Apparently, the Ph.D. journey is completely done. Let see what will come next, but I am now confident to look at other challenges as new milestones in life.

"*Hard work beats talent when talent doesn't work hard.*"
(Tim Notke, basketball coach)

Tokyo, March 2022
Tito Wijayanto

Contents

List of Tables

List of Figures

5

Glossary

agglomeration defines as a small or large group of many different things gathered into larger sizes. 4

core flooding defines as a laboratory test in which a fluid or combination of fluids is injected into a sample of rock. The objectives include measurement of permeability, relative permeability, saturation change, formation damage caused by the fluid injection, or interactions between the fluid and the rock. A core flooding is typically used to determine the optimum development option for an oil reservoir and often helps evaluate the effect of specially designed fluid injections to enhance or enhance oil recovery. 34

disjoining pressure defines as the attractive and repulsive force between two thin layers of fluid surfaces and occurs in ultra-thin liquid films. 15

enhanced oil recovery also called tertiary recovery, defines as a process for extracting oil that has not already been retrieved through the primary or secondary oil recovery techniques. 3

improved oil recovery defines as any of various methods, chiefly reservoir drive mechanisms and enhanced recover techniques, designed to improve the flow of hydrocarbons from the reservoir to the wellbore or to recover more oil after the primary and secondary methods (water and gas floods) are uneconomic. 3

interfacial tension defines as the tendency of an interface to become spherical to make its surface energy as low as possible. 3

nanofluids defines as suspensions of nanoparticles dispersed in a fluid base. 3

nanoparticles defines as any particles of a size within the range of 1–100 nanometers, also exhibit several unique properties of particulate material. 2

original oil in place defines as the amount of crude oil which is estimated to be in a reservoir. 12

permeability defines as a measure of the ability of the rock to transmit fluids and affected by the pressure in a rock. 18

porosity defines as the property of being porous and absorbing fluids and as the ratio of the volume of the voids or pore space divided by the total volume. The porosity of a rock depends on many factors, including the rock type and how the grains of a rock are arranged. 18

silanol defines as a functional group in silicon chemistry with Si-O-H connectivity. It is related to the hydroxy functional group (C-O-H) found in all alcohols. Silanol groups present in the fused silica capillary are readily ionized in the majority of conditions to form the negatively charged of the inner wall, which attract the positively charged components of the mixture to be separated.. 9

water flooding defines as a secondary recovery mechanism which involves the injection of water into the reservoir through injector well(s) to maintain reservoir pressure and drive the oil towards the producing well(s). 40

wettability defines as the capability of a liquid to keep connected with a solid surface. 30

Acronyms

APHA American Public Health Association. 25

API American Petroleum Institute. 25

ASP alkaline surfactant polymer. 13

ASTM American Society for Testing and Materials. 25

BOED barrels of oil equivalent per day. 1

CENT Center of Excellence in Nano Technology. 23

CMC critical micelle concentration. 39

DLVO Derjaguin, Landau, Verwey, and Overbeek. 10

e.g. exempli gratia (for example). 3

EOR enhanced oil recovery. 3

FW formation water. 25

HC hydrocarbon. 13

IFT interfacial tension. 3

IOR improved oil recovery. 3

ISO International Organization for Standardization. 8

KFUPM King Fahd University of Petroleum and Minerals. 23

MEMR Ministry of Energy and Mineral Resources. 1

MEOR microbial enhanced oil recovery. 13

MMP minimum miscibility pressure. 13

NFs nanofluids. 3

NNI National Nanotechnology Initiative. 2

NP nanoparticle. 4

NPs nanoparticles. 2

ppm part per million. 38

PV pore volume. 19

RP Recommended Practice. 26

rpm revolutions per minute. 33

SAGD steam assisted gravity drainage. 13

SB synthetic brine. 45

SG specific gravity. 26

SPE Society of Petroleum Engineers. 12

TAN total acid number. 25

TBN total base number. 25

TDS total dissolved solid. 25

TS Technical Specification. 8

TSS total suspended solid. 25

USBM United States Bureau of Mines. 22

WI wettability index. 30

XRF X-ray fluorescence. 26

Symbols

Greek Symbol

μ	Fluid viscosity	cP
μ_{w}	Viscosity of water	$kg/(m.s)$
$\mu_{\text{w,o}}$	Viscosity of water in oil phase	$kg/(m.s)$
σ	Interfacial tension	$dyne/cm$
ρ	Density of fluid	g/cm^3
$\rho_{\text{NP,w}}$	molar density of nanoparticles in water phase	mol/m^3
$\rho_{\text{o,o}}$	molar density of oil in oil phase	mol/m^3
$\rho_{\text{w,w}}$	molar density of water in water phase	mol/m^3
ω	Rotation speed	rpm
Π	Disjoining pressure	N/m^2
Δt	Time increment in time-step i	s
ϕ	Porosity	

Roman Symbol

AP	Possibility of agglomeration	
C	Concentration of nanoparticle	ppm
D_{NP_v}	Volume of nanoparticles dispersed in the liquid	m^3
E	Overall sweep efficiency	
E_{V}	Volumetric sweep efficiency	
E_{D}	Displacement efficiency	
I_{w}	Ratio of spontaneous saturation change to spontaneous plus driven saturation change for water	
I_{o}	Ratio of spontaneous saturation change to spontaneous plus driven saturation change for oil	
k	Absolute permeability	m^2
$k_{\text{rl}_{\text{no DP}}}$	Relative permeability to phase l at the stage where the disjoining pressure is not considered	
$k_{\text{rl}_{\text{no ads}}}$	Relative permeability to phase l at the stage where the adsorption of nanoparticles is not considered	

$k_{\text{rl}_{\text{max ads}}}$	Relative permeability to phase l where the full adsorption of nanoparticles is considered	mol/m^3
k_{ro}	Relative permeability of oil	
k_{rw}	Relative permeability of water	
M	Mobility ratio	
$_{\text{max}}N_{\text{NP}_{\text{Ads}}}$	Maximum number of moles of nanoparticles adsorbed on rock surface per unit bulk volume	mol/m^3
N_{NP}	Number of moles of nanoparticle in unit bulk volume	mol/m^3
N_{o}	Number of moles of oil in unit bulk volume	mol/m^3
N_{w}	Number of moles of water in unit bulk volume	mol/m^3
$N_{NP_{ads}}$	Number of moles of nanoparticles adsorbed on rock surface per unit bulk volume	mol/m^3
N_{C}	Capillary number	
P_o	Oil phase pressure	$kg/(m.s^2)$
P_w	Water phase pressure	$kg/(m.s^2)$
q_{NP}	Mole rate of injected nanoparticle per unit bulk volume	$mol/(m^3.s)$
q_{o}	Mole rate of injected oil per unit bulk volume	$mol/(m^3.s)$
q_{w}	Mole rate of injected water per unit bulk volume	$mol/(m^3.s)$
r	Effective radius of the interface	
S	Diameter of nanoparticle	nm
S_{oi}	Initial oil saturation	
S_{or}	Residual oil saturation	
S_{or_1}	Residual oil saturation before flooding	
S_{or_2}	Residual oil saturation after flooding	
$S_{\text{or}_{\text{no DP}}}$	Residual oil saturation at the stage where the disjoining pressure is not considered	
$S_{\text{or}_{\text{no ads}}}$	Residual oil saturation at the stage where the adsorption of nanoparticles is not considered	
$S_{\text{or}_{\text{max ads}}}$	Maximum residual oil saturation at the stage where full adsorption of the nanoparticles is considered	
$S_{\text{or}_{\text{max DP}}}$	Residual oil saturation expected at the maximum of the disjoining pressure	
S_{po}	Spontaneous oil saturation	
S_{pw}	Spontaneous water saturation	
S_{wi}	Initial water saturation	
t	Time	s
v	Fluid velocity	m/s
v_{r}	nanoparticle aggregation speed constant	$1/s$
$V_{\text{Agg}_{\text{total}}}$	Amount of nanoparticle aggregation up to time-step n	m^3
V_{ai}	Amount of nanoparticle aggregation at time-step i	m^3
V_{control}	Control volume	m^3
V_{i}	Volume ratio	
V_{pore}	Volume pore without aggregation of nanoparticle	m^3
x	One dimensional location	m

Chapter 1

Introduction

1.1 Background and motivation

Worldwide energy consumption has grown significantly spurred by sustainable economic growth and increasing demand in developing countries. Indonesia is the fourth most populous country in the world, with a population of over 250 million currently, it still classified as a developing country (DESA, 2019). According to Ministry of Energy and Mineral Resources (MEMR), Republic of Indonesia, as a developing country still depends on fossil energy, especially oil, which contributes to almost 32% of primary energy consumption (MEMR, 2018). The current oil field supply in Indonesia is reaching the stage of total declining production capacity (Hite and Bondor, 2004). Oil production in Indonesia is dominated by mature onshore fields experiencing rapid rates of decline, yet holding significant remaining reserves (Robson et al., 2005). The oil consumption in 2017 has reached 1.3 million barrels of oil equivalent per day (BOED), while oil production was 800,000 BOED (MEMR, 2018). As a consequence of that condition, Indonesia changed its status to an oil importer.

To offset this and provide solutions to this dilemma, the government encourages the oil operators to revitalize the brown-fields through improved oil recovery, both from a feasible economic standpoint and in an environmentally

friendly method. New technological advancements are needed in order to be able to extract more oil from these mature oil fields, amongst them is nanotechnology that can help achieving this goal. Nanotechnology has the potential of changing the way of petroleum exploration and production, and is tackled in both the upstream and downstream industries. This technology provides various alternatives for the materials, and it is handling its execution and workflow that will be applied to the modernized petroleum industry.

As claimed by the National Nanotechnology Initiative (NNI), the nanotechnology, as defined by size, is the material manipulation, where the nanomaterial is at least one dimensional, and its size varies from 1 to 100 nanometers (10^{-9}m) (Dunphy Guzmán et al., 2006). Research and related applications vary widely, from the expansion of ordinary device physics to truly novel advances based on atomic self-assemble. Moreover, evolving unique substances with proportions at the nano-sized to straightforward control of individual on the subatomic proportion was pursued (Belkin et al., 2015). Nanotechnology is maybe capable of creating various elements and appliances with various utilizations usages. However, the future of inference on its utilization is still a debatable stage due to various issues, amongst others, such as toxicity and environmental impact.

The study of nanotechnology has been growing and has dragged the courtesy to develop state-of-the-art keys to fulfill the requirement for oil. Barron (2010) has concluded that nanotechnology would become a much more common term within the oil and gas industries in the next decade. Nanoparticles (NPs), which is as part of the nanotechnology contrivance, offer several benefits, such that they are environmentally friendly and can be tailored to meet specific reservoir conditions as well as it offers a reasonable degree of control manipulation of its physical-chemistry properties (Miranda et al., 2012). Another benefit of adopting NPs is that the dimensions are much lesser than the frequent reservoir pore throat. Therefore they can propagate in reservoir rocks. Kong and Ohadi (2010) highlighted that NPs, with size typically less than 100 nanometers, are po-

tentially applied for many disciplines, including the oil and gas industry. Previous studies reported that NPs are advantageous for enhanced oil recovery (EOR) purposes, the NPs first need to be converted to nanofluids (NFs) before its usage (Das et al., 2007). Rao (2010) and Das et al. (2007) determined that NFs are suspensions of NPs dispersed in a fluid base (e.g., water, oil, or a conventional fluid mixture). Many studies have described NPs usages in the field of improved oil recovery (IOR) methodology as well as EOR (Buongiorno, 2006). Cheraghian et al. (2017), Li and Torsæter (2014), Zargartalebi et al. (2014), Hendraningrat et al. (2013a), Ogolo et al. (2012) and Miranda et al. (2012) applied silica-based NPs to reveal its the potential for a novel EOR, while Mahbubul et al. (2014) and Giraldo et al. (2013) applied alumina-based NPs. They investigated the displacement mechanism, mainly focusing on changes in wettability and the decreasing of interfacial tension (IFT). These established results suggested the potential NPs for the EOR application and usages.

For example, silica-based NPs, inorganic materials, are more easily produced because silicon dioxide (SiO_2) is one of the amplest families of harmless components, existing as both natural minerals and those produced synthetically. These silica-based NPs also have an adaptive control, manipulating their physical-chemical properties, and efficiently functioning from hydrophobic to hydrophilic with silanization. While alumina-based NPs are chemically stable, it has increased mechanical strength and as an electrically insulating material. Even though Metin et al. (2012) opined that NPs have a low cost of fabrication, the economic cost of applying nanotechnology for the EOR method remains unknown due to the fact that most experiments worldwide are still investigating these cost factors while conducting their research and development of this nanotechnology for the EOR.

Based on the contrary facts and the reasons mentioned in the previous paragraph, the ultimate purpose of this research is to substantiate the applicability of NPs and evaluate the performance of NPs as one of the emerging technology in EOR methods at the laboratory scale before field deployment.

1.2 Problem formulation

Over the past decade, most commonly used silica-based and alumina-based NPs investigations offer promise for the EOR processes. Meanwhile, the concept of the oil displacement mechanism by NPs remains unclear. In this thesis, laboratory experiments were designed to obtain a fundamental concept of how NPs displace remaining oil in porous media and to unlock the potential of NPs as new EOR agents.

NFs are novel class engineered liquid and contains a two-phase structure, solid and liquid. NFs are NPs dispersed in a base liquid. Hence, the stability of NFs is a significant issue (Das et al., 2007). To provide the desired stability of NFs over time and across temperatures is a considerable challenge (Xie et al., 2010). In this thesis, laboratory observations are described to investigate a process to enhance the stability of aluminosilicate NPs in brine and its effect on EOR processes. Almost all the previous research considered the response of the NFs from the viewpoints of wettability and IFT. However, in those researches, the nanoparticle (NP) suspensions were constructed not merely by pure NPs, yet consisted of the surfactants or stabilizers to avoid agglomeration, which may have influenced the wettability and IFT, and made it uncertain which parts in the NP suspensions played a vital role.

With a limited period of a doctoral program and laboratory instruments, some parameters are studied, not using any stabilizer agents for solving ambiguities as well as minimizing costs. This research used synthetic brine, synthetic oil, formation water, and crude oil from the field (Langgak Field in Indonesia), which can be an option to increase Indonesia's oil production.

1.3 Objective of the research

The ultimate objective of this research is to substantiate the applicability and evaluate the performance of NPs as one of the emerging technology in EOR methods at lab scale before field deployment. Whereas the specific objectives are described from reservoir engineering points of view, as follows:

(1) To characterize the nanomaterials employed in all experiments, which consists of the NPs, crude oil, NFs, and porous media (core plug).

(2) To characterize silica-alumina-based nanomaterial for nano-EOR from viewpoints of stability, IFT, and wettability.

(3) To conduct a two-phase core flooding test for clarifying dynamic fluid-rock interaction.

(4) To investigate the displacement mechanism by NPs.

1.4 Outline of the thesis

The synopsis of the thesis is as follows:

Chapter 1 provides a brief background and motivation for this thesis, and also an overview of NPs. The problem statement is defined, and also the scope of the work is described.

Chapter 2 describes the theoretical background and fundamentals of NPs in EOR, including relevant aspects and parameters to be investigated. Liquid-liquid and liquid-rock interactions are also presented to reveal possible displacement mechanisms using NPs, such as wettability alteration and IFT.

Chapter 3 contains an explanation of the materials and their characterization, also the methods and procedure for all experiments involved in liquid behavior, liquid-liquid, and liquid-rock interactions on account of the presence of NPs. The laboratory experiments covered stability investigation, wettability determination

using the Amott-Harvey methods, IFT measurement, and the displacement test. This chapter presents the first publication.

Chapter 4 provides the setup and procedures of the experiments, which covered IFT analysis, wettability determination using the contact angle method, and the core flooding test. This chapter presents the second publication.

Chapter 5 describes numerical simulation, with governing and constitutive equations, conducted to examine the oil displacement mechanisms expected in nano-EOR quantitatively.

Chapter 6 summarizes the overall conclusions and recommendations for further research.

Chapter 2

Theoretical background

This chapter presents the fundamental concepts and definitions relating to NPs and NFs, also shown the illustration of NPs and followed by the current excerpts of results from the literature of NFs and its applications in NFs and its applications in IOR/EOR.

2.1 Nanotechnology

The nanotechnology concept was initially discussed in an Engineering and Science magazine authored by a well-known physicist, Richard Feynman (Feynman, 1959). The term nanotechnology was first used to express semiconductor developments in a nanometer in a substance on work conducted by Norio Taniguchi (Taniguchi, 1974). Nanotechnology knowledge was further promoted when carbon nanotubes were established by Iijima (1991). The term nanotechnology is now described as the manufacture of purposeful components, appliances, and arrangements where handling the matter is conducted at the nanoscale zone and utilizing their source characteristics and circumstances appears on their system (Das et al., 2007). While in accordance with Drexler (2001), nanotechnology is defined as manipulating content on an atomic, molecular, and supramolecular level. The length of ordinary carbon-carbon bonds or the imbalance between

atoms in a molecule is illustrated in Figure 2.1a by Wichlab of the University of New South Wales, Australia. Kong and Ohadi (2010) and Mokhatab et al. (2006) stated that nanotechnologies have evolved into the petroleum industry in recent years, including geochemical investigation, drilling, sand problems, and heavy oil development as well as reservoir engineering.

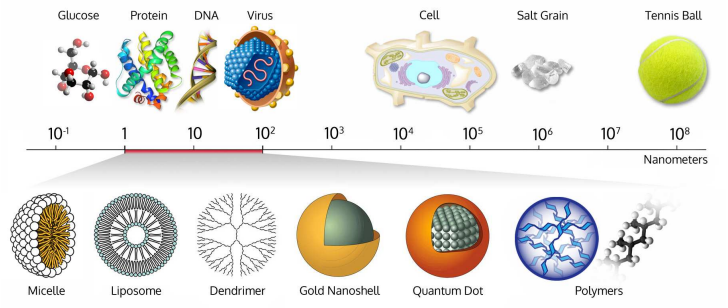

(a) Nano-materials sizes (Illustrated by Wichlab of University of New South Wales).

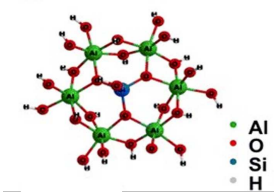

(b) Structure of silica-alumina-based NPs (Modified from (Baroña et al., 2013)).

Figure 2.1. Comparison of nano-material and an example of structure of NPs.

2.1.1 Nanoparticles

The NP usually refers to inorganic materials, which are not applied to individual molecules, and its definition is any particle of a size within the range of 1–100 nanometer that exhibits several unique properties of particulate materials (Vert et al., 2012; Feynman, 1959). While referring to the International Organization for Standardization/Technical Specification (ISO/TS) 80004, NP is defined as a nano-object that employs sizes and geometric boundaries that express the fundamental and measurable aspects of nanomaterials. In contrast, the nanoscale is defined as the actual size range of nano-objects that may fall outside the precise boundaries (ISO, 2007). Because of their size, the NPs have unique material characteristics that can be produced for practical applications in multiple fields, such as medicine, engineering, catalysis, and environmental improvement.

The NPs can be categorized into different classifications based on size, shape as well as material characteristics. Classifications are identified within organic and inorganic NPs; the first classification is those that include dendrimers,

liposomes, and polymeric NPs, while the following classification includes fullerenes, quantum dots, and gold NPs. Also, for comparison, the size of NPs is a million times smaller than a tennis ball (Figure 2.1a). Besides these classifications, NPs could be listed as hard or as soft silica particles. Silica NPs have a single and geminal silanol (silicon chemistry with the connectivity Si–O–H) group, and silanol is more acidic than other alcohols. The structure of single and geminal silanol groups in NPs is shown in Figure 2.1b. The general method in which NPs are classified typically relies on the purpose. The purpose is in an investigation and/or possibly linked to how the NPs were assembled. According to Jarvie et al. (2019), the NPs have three main physical properties, and they are all interrelated. Firstly, the NPs are very movable in their free-state condition (e.g., a 10 nm width silica nanosphere has an agglomeration velocity below 0.01 mm/day in water) without any additional influence. Secondly, these NPs have a vast specific surface area (e.g., one regular teaspoon or approximately 6 ml, a 10 nm width silica nanosphere has a surface field-area of more than a dozen tennis arenas; 20 percent of molecules in each nanosphere will be positioned at the surface). Thirdly, the NPs can show what is known as a quantum effect. Thus, NPs can be characterized as having various compositions, dependent on their usage or product. The NPs that were obtained were recognized and showed to possess excellent standardized and thermal stability. It was shown that they could be tailored to comply with the particular targeted reservoir environment, such as wettability, mobility ratio, or manage formations and fines migration (Andreassen, 2015). Zhang et al. (2014) concluded to optimize the properties of NFs, for example, thermal conductivity, viscosity, and specific heat.

2.1.2 Nanofluids

NFs are a novel class of engineered liquid that contains nanometer-sized particles generated by nanoscience, nanotechnology, and engineering collaboration, making it an important new interdisciplinary area (Yu and Xie, 2012). Also, NFs are

defined as liquid suspension of dilute NP, which represents a class of colloidal mixes containing nanometer-sized particles such as metal or non-metal oxides, carbides, ceramics, carbon, as well as mixtures of different NPs (hybrid NPs) and even nanoscale liquid droplets. The NFs are soluted in a conventional liquid that conducts heat (e.g., oil, water, or a conventional fluid mixture) that forms a colloidal suspension (Rao, 2010; Das et al., 2007). NFs have many capabilities to advance and innovative properties that are possibly useful in countless utilization (Minkowycz et al., 2016). The utilization of NFs for oil and gas application is summarized in Table 2.1 (Kong and Ohadi, 2010).

Table 2.1. The potential of NFs application in the petroleum industries.

Purpose	**Area**
The exploration success ratio is improved by increasing data collection, dodging dry holes, and identifying shallow hazards	Exploration
The increasing material strength and durability, therefore the performance and reliability in drilling, tubular goods, and rotating parts, improved pH (4-5 % in dispersion)	Drilling
Guaranteed production in diagnostics, supervision, and supervision strategies	Production
Surface, subsurface, and facility application's corrosion management	Facilities
Refinement and petrochemical-based technologies	Downstream
Improved oil and gas recovery through modification of reservoir properties, gas, and water injection modification	Reservoir

The stability of NFs is crucial for engineering applications such as EOR. The NFs are easily aggregated after dehydration, and this occurs because it has a large ratio between its surface and its volume as a consequence of a large molecule size (Keller et al., 2010). The NPs held high surface energies, and the materials with a large surface-to-volume ratio reacted much faster. Therefore, they tend to agglomerate. Controlling this energy is a critical issue to ensure that the particles remain discrete and as small as their original size. The Derjaguin, Landau, Verwey, and Overbeek (DLVO) concept explained that the NP aggregation is the formation of clusters by particles, or when small clusters aggregate to form larger

ones due to the balance of forces in the system (Figure 2.2) (Druetta and Picchioni, 2019). This concept is best suited for describing colloidal cohesion and holding the tension between two contradictory forces, attractive and electrostatic repulsion forces. The electrostatic repulsion force converts significantly when two colloids contact one another. Also, this concept clarifies the trend of solutions to agglomerate or to remain distinct. The point of maximum repulsive force is called the energy barrier. The system will be more stable if the barrier is high (Rao, 2010).

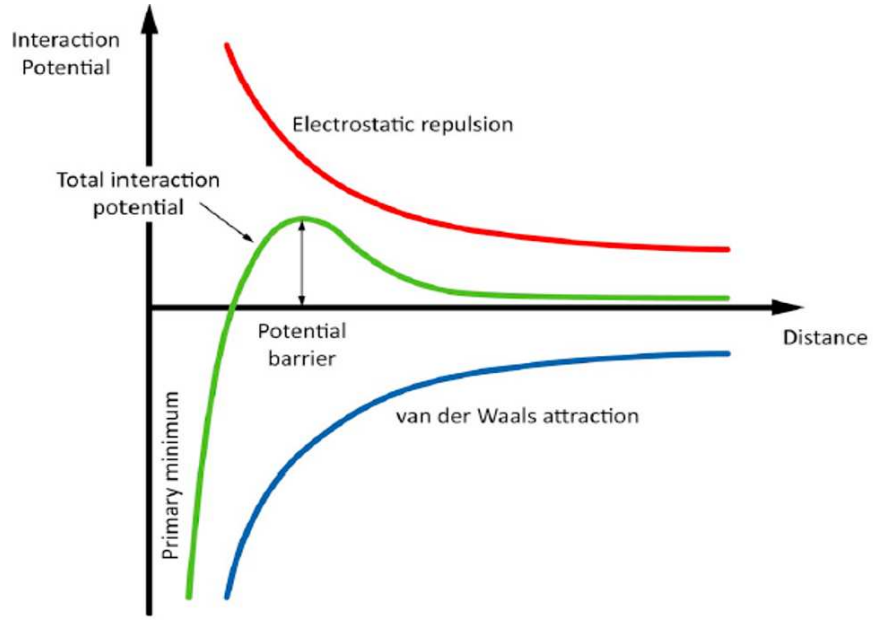

Figure 2.2. The forces at the molecular scale that affects the NPs.

Yu and Xie (2012) classified the preparation of NFs into two procedures: a one-stage procedure consists of producing and spreading NPs synchronously in the base liquid, it can be prepared for the NPs to disperse uniformly can be firmly suspended in the base liquid. In this procedure, the agglomeration of the NPs are reduced because it avoids long processes, though the disadvantages of this procedure are high cost, and it cannot be synthesized on a large scale. A two-stage procedure is the most universally applicable procedure for NFs formulation. First, the NPs are prepared as a dry powder, and this dry powder is spread into a base liquid with frequent agitation. Agitation such as intense electromagnetic, ultrasonic, high-shear blending, and a ball grinding mill usage. The advantage of using this

two-step procedure is that it is much cheaper than the one-step procedure. In this thesis, the two-step procedure is applied to prepare the NFs, and the proceeding will be explained in Chapter 3.

2.2 Nanofluids for EOR

As mentioned in Chapter 1, global energy consumption and demand increase while oil production is declining. They are also facing increasing field abandonment of oil fields with capacities exceeding 50% of the original oil in place (OOIP) unrecovered (Fletcher and Davis, 2010). The ultimate challenge now is how to minimize the gap between consumption and production through methodology on how to increase the recovery factors from mature fields economically and in an environmentally friendly manner.

Lake (1989) stated that EOR as oil recovery through the injection of materials not present in the reservoir. The Society of Petroleum Engineers (SPE) stated that IOR also consists of EOR. Primary recovery and IOR (secondary and tertiary recovery) methods follow the natural progression of oil production. EOR process requires the injection of chemical compounds dissolved in water, or steam injection, or gas injection. Thus, all current EOR processes are much more expensive than secondary recovery, water injection method. Therefore, the IOR/EOR methods contribute to economic indices, such as oil prices, capital expenditures, and operational expenditures. The era of ”easy” oil has vanished, and new significant discoveries are becoming rare and more expensive, such as immobile and heavy oils, as well as deep-sea reserves. Based on these facts, EOR methods play crucial roles in the recovery of immobile oil. The EOR methods, such as thermal, chemical, and miscible flooding, have their challenges, as shown in Table 2.2 (Hendraningrat, 2015).

Table 2.2. EOR methods, mechanisms and challenges.

Method	Mechanism	Challenges
Thermal		
Steam injection, steam assisted gravity drainage (SAGD), in-situ combustion	IFT reduction, oil expansion, viscosity reduction, steam distillation	High cost per incremental barrel of oil; low thermal conductivity of rock and fluids; heat leakage to the undesired layer; low sufficient thermal; wellbore damage due to initial high temperature; heat loss from heat generator to the reservoir
Chemical		
Alkaline surfactant polymer (ASP), and combination	Wettability alteration, IFT reduction, mobility control	High cost; low effectiveness on IFT and viscosity; damage due to incompatibility; unfavorable of mobility ratio; slow diffusion rate in pore structure; an unknown mechanism for wettability alteration
Gas injection		
Miscible and immiscible (hydrocarbon (HC) gas injection, CO_2 injection, air injection)	Viscosity reduction, pressure maintenance, oil expansion, miscibility	Gas low viscosity leads to fingering, and early breakthrough; high minimum miscibility pressure (MMP) needed to have miscible flooding for higher recovery efficiency; in case of CO_2 corrosive resistance materials are needed; side effects such as asphaltene deposition occurs
Microbial-EOR (MEOR)		
Nutrition injection, bioproducts	Oil biodegradation, selective plugging, wettability alteration, IFT reduction	The very slow mechanism; undesired plugging; bioreactions; nutrition delivery to the microorganism and chemically assisted MEOR

2.2.1 Literature Review

The usable of NPs in EOR has several benefits, such as being cheap and environmentally friendly; NPs can be easily modified to enhance its desirable properties, such as wettability alteration, increased mobility, reduced IFT and control of the formation fines migration; NPs have a low capital cost for installation; NPs can move through porous media without plugging pore throats; metallic NPs can be separated from oil using magnetic separation; NPs could be selected to expand the viscosity of displacing liquid, thus decreasing mobility of displacing liquid and avoiding viscous fingering in the process; NPs are capable of modifying oil/water

interfacial tension; NPs have a significant ratio of surface region to volume, which results in improved thermal properties; NPs generate a wedge film or structural disjoining pressure which remove oil droplets from the rock; NPs and nano-gels can be used for selectively plugging water paths thus driving the water to stream through oil-filled paths (Aurand, 2015; Khan and Rizvi, 2014; Cheraghian et al., 2013; Metin et al., 2012; Miranda et al., 2012).

NPs possess particular characteristics due to their molecule sizes and a larger ratio of the surface area to volume and have high adsorption correspondence (Ehtesabi et al., 2013). Also, NPs are composed of core and thin shells, and they might become original compositions and formed of several substances (Das et al., 2007). The surface movement from NPs impressed by the diffusion stability of the NPs in solution and usually treated or functioned, thus placing the shield around them. This shield inhibits the interaction of particles and the possibility of reduced agglomeration of NPs. The NP may alter the reservoir liquid configuration and rock-fluid characteristics to support in assembling confined oil. This assistance may contain several physical or chemical contacts that may lead to effective displacement mechanisms with small residual saturation.

The number of publications related to NFs for the IOR/EOR topic continuously increases, showing the potential on a laboratory scale. Previous research by Cheraghian et al. (2017), Zargartalebi et al. (2014), and Hendraningrat et al. (2013a) showed that the silica-based NPs affect wettability. Whereas according to Ogolo et al. (2012), they stated that it was most efficient in changing rock wettability and reducing oil viscosity when dispersed in brine, also the sufficient is for trapping and migrating in fine sand.

2.2.2 Recovery Mechanism

The conventional EOR recovery mechanism focuses on capillary, viscous, and gravity forces. However, the past works have identified the recovery mechanism of NFs, such as wettability alteration of rock surface, IFT reduction, dis-

joining pressure, and pore channel plugging (Kazemzadeh et al., 2019; Agista et al., 2018). Morrow (1990) stated that wettability plays a critical part in oil recovery and resolves the recovery efficiency of displacement processes. Wettability affects both the distribution of oleic and aqueous phases within the rock matrix and the dynamics of displacement processes. Buckley and Fan (2007) concluded that the IFT affects the capillary number and pressure, adhesive force, and non-dimensional period for imbibition. The capillary number expanded with the reduction of the IFT value, and therefore, the remaining oil was organized. By reducing the IFT value and altering the rock wettability, the capillary pressure will decrease and improve the oil recovery. Figure 2.3 and figure 2.4 are the conceptual diagrams of IFT between NPs-brine and oil on the effect of IFT reduction, and making water film on a solid surface by NPs on the impact of wettability alteration, respectively.

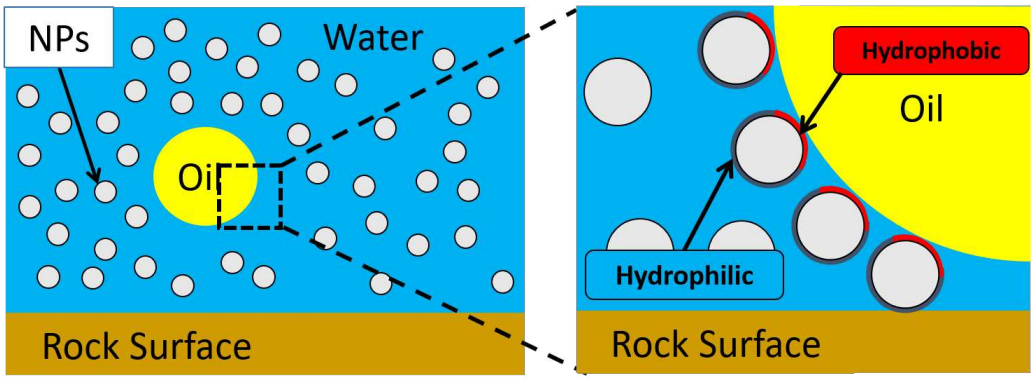

Figure 2.3. The conceptual diagram of IFT between NPs and oil on the effect of reducing the IFT values.

The disjoining pressure is described as the attractive and repulsive force amongst two liquid surface layers and only occurs in thin liquid films. Once ultra-thin liquid films interact with a rock surface, this results in a reaction between the liquid and solid molecules. The liquid force must balance the surrounding energy and attractive force among the liquid and solid (Faghri and Zhang, 2006). The disjoining pressure generated changes the thermodynamic stability conditions at the steam-liquid boundary of thin films. The structural disjoined pressure corre-

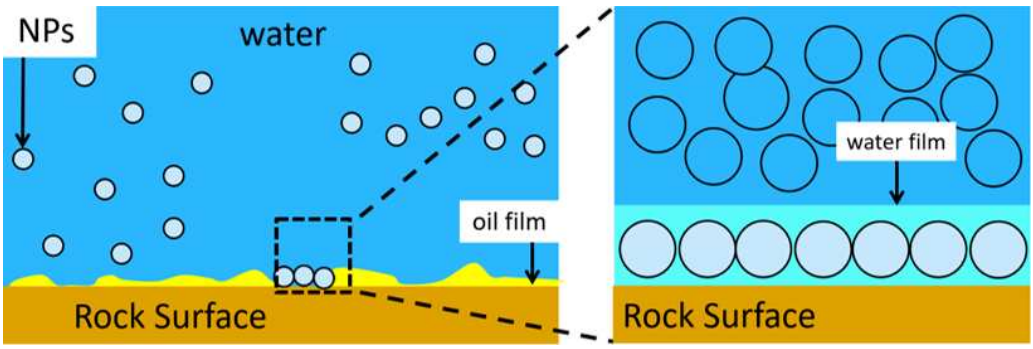

Figure 2.4. The conceptual diagram of making water film on a rock surface by NPs on the effect of wettability alteration.

lates through the liquid ability to disperse toward the substrate surface due to the inequity of the IFT among solid (rocks), oil, and aqueous phase (Chengara et al., 2004). This pressure conforming to the one-layer-film thickness of the particle is observed to be higher than the two-layer-film (wedge-shaped film), and the conceptual diagram showing the effect of NFs on structuring a disjoining pressure is presented in Figure 2.5.

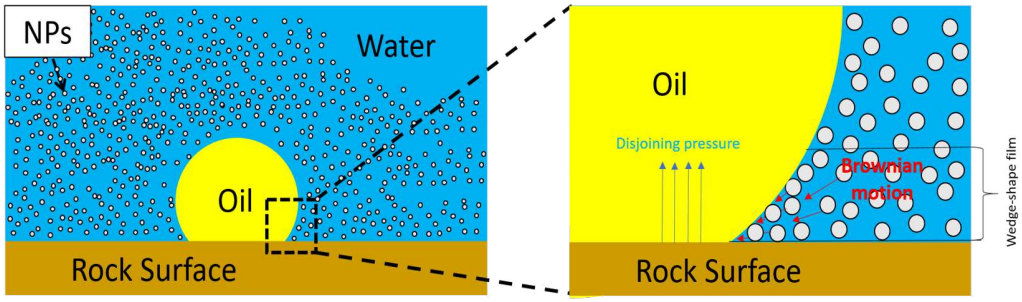

Figure 2.5. The conceptual NPs structuring in wedge-film is resulting in structural disjoining pressure gradient at the wedge vertex (modified from Wasan et al. (2011)).

The width of the structure is resolved by an equilibrium between Van der Waals' attractive and electrostatic repulsion force (Keller et al., 2010). The mechanisms that cause these forces are Brownian motion and electrostatic repulsion forces (Afekare et al., 2020; Sofla et al., 2018). When NPs are hydrated, they tend to agglomerate. Thus, they have abundant energy and alter the structure of wettability (Giraldo et al., 2013) and accordingly generate into a collective form to minimize this surface energy (Wu et al., 2008). Based on this mechanism, the

disjoining force is responsible for releasing oil from the rocks while permitting the NFs to spread further. Hendraningrat et al. (2013b) stated that increasing the structural disjoining pressure mechanisms is the effect of wettability alteration and reduced the IFT. While according to Adil et al. (2020) and Zhang et al. (2018), the disjoining pressure increases the oil displacement from rock surfaces when compared to the conservative method without adding the NPs.

Mechanical entrapment and log-jamming are the mechanisms of pore channel pugging effects. The mechanical entrapment may occur if the width of NPs is higher than the pore networks and only comes into play when there is a presence of metal NPs while the log-jamming mechanism works when NFs flow from the pores to pore-throats, where it is caused by the change of channel diameter and resulting pressure differences, that leads to acceleration of NFs flow. The liquids molecules will flow faster than the NPs due to their smaller size, while the larger and slower NPs will accumulate at the entrance of the pore throat, leading to channel plugging. The density gradient decelerates the flow of the particles through the winding sections within the rock, and the particles assemble and consolidate at blockage points to clog the rock pores. The pressure in adjacent pores discharges the oil (showing in green in Figure 2.6), and the surrounding pressure drops when the oil is released, the barrier gradually dissolves, and the NPs commence flowing with the water. The conceptual diagram for the pore channel plugging mechanism is illustrated in Figure 2.6 by the Center for Integrated Petroleum Research, Norway.

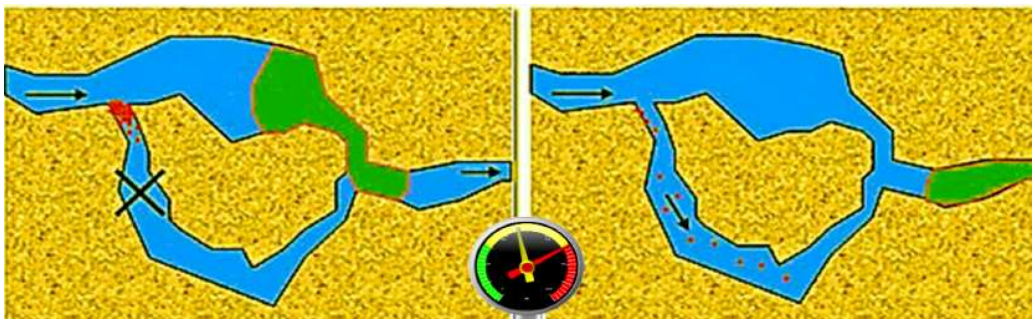

Figure 2.6. The conceptual diagram for pore channel plugging mechanism.

Silica-based NPs could act as log-jamming proxies when the silica did not amass in the oil when dispersed in brine, while it gathers at the pore-throat inlet, and encompass a specific viscosity to overcome the local threshold of oil flow (Skauge et al., 2010). This approach is based on encouraging water injection with substantially smaller particles than the rock pore diameters. When water-enhanced particles reach the channel hole, they will advance faster than the particles, leaving them behind to assemble and plug the pore entrance, essentially sealing the pore.

2.3 Relevant Reservoir Parameters

2.3.1 Rock and Fluid Properties

Porosity and permeability are the two essentials of rock properties in reservoir engineering and pressure functions. They regulate rock storage capacity and spatial distribution, conduct fluids, and affect their spatial and directional distributions. The definition of porosity is the pore ratio to bulk rock volume and is generally expressed as a percentage (White, 2012). Also, porosity is the substance of a rock storage quantity. Effective porosity is defined as fluid flow through rocks or sediments and is most widely examined to represent the porosity of the rocks. It is very significant to consider the compatibility of rocks or sediments in oil or gas reservoirs or aquifers.

Permeability is defined as the substance of a rock's capability to diffuse fluids and is influenced by a rock's pressure. Permeability is a crucial variable that controls the distribution of transient conditions asserted at the well. Permeability is a part of Darcy's law that connects the movement velocity and liquid physical characteristics (e.g., viscosity) with a forced angle applied to porous media. The permeability theory is essential in defining HC flow features in oil and gas reservoirs (Guerriero et al., 2013). Both porosity and permeability are func-

tions of pressure.

Similar to rock properties, fluid properties might dramatically influence the motion of fluid movements in porous media. Fluid properties are pressure-dependent. For instance, the oil properties that appear in the flow equation governing the oil phase are density, compressibility, viscosity, gas solubility, and formation volume factor. The essence of this oil can be preserved presented as a constant when the gas phase is not present because the compressibility of gas-free oil is considered a minor factor. However, the presence of dispersed gases in said oil requires harmonious relationships criteria to control variations in these properties.

Another property that should be considered is saturation. Saturation is represented as the portion of the pore volume (PV) occupied by a specific fluid (oil, gas, or water). The residual oil saturation value is categorized among vital considerations in advance of EOR as it represents the immobile oil left in the reservoir. The assumption of the summation of oil, gas, and water saturation equals one if three phases initially exist in a reservoir. The saturation of a specific fluid (oil, gas, or water), denoted as S_i, is represented as the volume ratio (V_i) to the PV and is formulated as follows:

$$S_i = \frac{V_i}{PV} \tag{2.1}$$

2.3.2 Displacement Efficiency

Any EOR processes commence with investigating the origin and place and induce residual oil saturation (S_{or}) that persists after primary and or secondary recovery processes. The aspects that control the S_{or} value are pore geometry, rock wettability, and the displaced oil and injected fluid characteristics. The fluid properties of unique concern are IFT, viscosity, and density. All EOR projects depend on macroscopic and microscopic sweep efficiencies. Green and Willhite (1998) defined volumetric sweep efficiency (E_V) as macroscopic sweep efficiency and displacement sweep efficiency (E_D) as the microscopic sweep efficiency. The

overall sweep efficiency (E) is formulated as follows:

$$E = E_{\mathrm{V}}.E_{\mathrm{D}} \tag{2.2}$$

The microscopic sweep efficiency is conversely comparative to the mobility ratio (M) between the injected fluids and the oil in place, while displacement efficiency is inversely proportional to the residual oil saturation. M is defined as a fluid phase movement (k_r) divided by the phase viscosity (μ) to the same ratio for the other phase. In conventional terms, the detection of incremental oil recovery for EOR decreases in choosing the process that minimizes M or S_{or} for a typical reservoir.

The macroscopic level involves the areal and vertical sweep efficiency and might be affected by fluid differences and reservoir rock heterogeneity. In contrast, the microscopic displacement efficiency shows the fluid transfer that mobilizes the oil and is influenced by the interaction involving the capillary pressure, IFT, wettability, capillary pressure, and relative permeability. At the microscopic level, the forces are mainly the viscous and capillary forces. One of the primary goals in an EOR process is to enlarge the capillary number (N_C) (Amziane and Collet, 2017). It is represented the ratio of viscous force to surface strain forces substitute cross-ways a boundary between two immiscible liquids, and it can be expressed as:

$$N_{\mathrm{C}} = \frac{\mu.v}{\sigma} \tag{2.3}$$

where μ is fluid viscosity, v is fluid velocity, and σ is IFT.

Displacement sweep efficiency (displacement efficiency) defines oil recovery as a consequence of the wettability effect, which characterizes how the S_{or} is efficiently reduced (Morrow, 1990), and it can be expressed in Equation 2.4.

$$E_{\mathrm{D}} = \left(1 - \frac{S_{\mathrm{or}_2}}{S_{\mathrm{or}_1}}\right) \tag{2.4}$$

where S_{or_1} is the S_{or} before flooding, and S_{or_2} is S_{or} after flooding.

2.3.3 Interfacial Tension

The primary fluids in a petroleum reservoir are oil, gas, and water, commonly in immiscible conditions. Whenever these immiscible fluids co-exist in the porous media (rock pore space), their interactions will occur and control the spatial distribution and movement in the rock pore space. The property used to quantify the interactions between two primary fluids is IFT. IFT is defined as the force that holds the surface of the specific phase together and must be examined to determine its significance for oil recovery. When the system consists of three phases (oleic, aqueous, and solid), the contact between these fluids and between the fluid and the solid has a particular IFT value. IFT is the tendency of an interface to become spherical to make its surface energy as low as possible.

The surface energy phenomenon is significant in oil recovery, particularly in EOR processes, which is mainly based on altering the surface energy to favor oil recovery. Oil recovery is directly correlated to capillary number (Amziane and Collet, 2017). This correlation is explained as a fraction of adhesive thrust to capillary thrusts responding to an alliance among fluid and gas or within two immiscible fluids (Green and Willhite, 1998). Green and Willhite (1998) stated that fluid process effectiveness in removing oil from rocks at the microscopic scale is a significant aspect of each EOR process. There are several IFT measurements methods: the Du Nouy ring, Du Nouy-Padday, pendant drop, Wilhelmy plate, bubble pressure, drop volume, capillary rise, stalagmometric, sessile drop, levitated drop, and spinning drop method (Drelich et al., 2002).

2.3.4 Wettability

Reservoir fluid flow is generated by complicated interactions between the reservoir rocks and fluids. Due to complications from the porous structure and mine-

ralogy of the reservoir rock, these complicated interactions are present in the same pore (Morrow, 1990). Wettability of particular liquid preference preserving interaction with a rock surface resulting from contact between molecules when they joined. Wettability is specified by the stability of the forces between adhesion and cohesion forces. Wettability is related to three phases of material: liquid, gas, and solid, and is essential through adherence instead of coupling two elements. The wettability and IFT are responsible for the impact and associated capillaries (Amziane and Collet, 2017). Hence, understanding the relationship between capillary pressure, wettability, and the arrangement of oil and water in the pore network is essential to improving oil recovery and has become an obligatory phase in the difficult task of measuring wettability.

Wettability influences the relative permeability, which supervises the movement and spreading of liquids in porous media. Nevertheless, wettability is not an individual variable that dominates relative permeability. Anderson (1987) concluded that relative permeability is induced by saturation, saturation history, geometric pore shape, and liquid distribution. Thus, wettability confirmation and its influence on oil by designs concerning core samples will be connected to further core interpretation (Morrow, 1990). There are numerous procedures to quantify a reservoir wettability, such as contact angle determination (Anderson, 1987), electrical resistivity (Sondenaa et al., 1991; Marsden et al., 1973; Morgan and Pirson, 1964), United States Bureau of Mines (USBM) method (Donaldson et al., 1969), Amott and Amott-Harvey method (Amott, 1959).

Chapter 3

Aluminosilicate nanoparticles for EOR agent

This chapter describes the method and procedure for all experiments that covered stability investigation, wettability index determination using the Amott-Harvey methods, IFT measurement, and the core flooding test. This chapter presents the first publication titled *Experimental Investigation of Aluminosilicate Nanoparticles for Enhanced Recovery of Waxy Crude Oil*.

3.1 Materials for the experiment

3.1.1 Nanoparticles

The powder form hydrophilic silica-alumina-based NPs, aluminosilicate with the chemical formula $(Na_2Ca_2K_2)_4(H_2O)_{28}(Al_8Si_{40}O_{96})$ as the main nanomaterial was used in this research and Figure 2.1b is illustrated the structure of silica-alumina-based NPs. The NPs are prepared and provided by the Center of Excellence in Nano Technology (CENT), King Fahd University of Petroleum and Minerals (KFUPM), Kingdom of Saudi Arabia. The aluminosilicate NPs properties are presented in Table 3.1.

Table 3.1. The properties of aluminosilicate NPs.

Properties	**Unit**	**Value**
Particle size	nm	90
Surface area	m^2/g	83
Surface area	m^2/g	65
Micropore area	m^2/g	18
Composition:		
- Al_2O_3	wt%	5.48
- SiO_2	wt%	52.52
- P_2O_5	wt%	0.51
- K_2O	wt%	0.53
- CaO	wt%	2.90
- TiO_2	wt%	0.27
- Fe_2O_3	wt%	1.49
- ZrO_2	wt%	0.72

Since the primary nanomaterial contains silica and alumina, it has the benefit of combining silica and alumina. Thus, Miranda et al. (2012) described that the benefit of silica-based NPs is more accessible to produce, it has a reasonable degree of control manipulation of their physical-chemical properties, and is easily surface-functionalized from hydrophobic to hydrophilic by silanization. They are one of the veriest affluent non-toxic materials. Metin et al. (2012) stated that silica-based NPs have a low cost of fabrication. While Ogolo et al. (2012) concluded that alumina is recognized as the most efficient NPs for migrating and capturing in fine sand compared to other metal oxides NPs. According to Giraldo et al. (2013), the adsorptive of alumina-based NPs could modify the wettability throughout its layer mechanism.

3.1.2 Fluids

3.1.2.1 Crude oil

Crude oil is oil in its original state before it is processed or purified and consists of HC deposits and other organic materials. While according to Investopedia, crude oil is a spontaneously appearing, crude petroleum commodity formed of HC stakes and other organic materials (Chen, James, 2019). Paraffinic crude oil

with an asphaltene content of around 25 wt% is retrieved from Langgak field in Indonesia and was used as an oleic base in this research. The total acid number (TAN) and base number (TBN) of the crude oil were measured at the laboratory condition base using a titration system-based, and the properties are shown in Table 3.2. The TAN and TBN are the standard procedures by American Society for Testing and Materials (ASTM) (ASTM, 1995, 2011).

Table 3.2. The properties of crude oil.

Properties	**Unit**	**Value**
TAN	mg KOH/g	0.499
TBN	mg KOH/g	2.656
Density @ 60 °C	g/cm^3	0.8702
Viscosity @ 60 °C	cP	19.97
Oil gravity	API	30.9

3.1.2.2 Formation water

Formation water (FW) is defined as the water that exists naturally in rocks and occurs spontaneously in sedimentary rock pores. It is water-related with the oil and gas reservoir and has some extraordinary chemical substances (Wan, 2011). FW can transfer to appropriate fluid dynamic environments. During HC creation, the FW can be created simultaneously with HC and referred to as the water cut. FW has chemical and physical properties (e.g., composition, salinity) that can show significant and unique variations. FW comprises dissolved and non-dissolved oil/organics, suspended solids, soluble solids, and various chemicals used in the production procedure. FW was retrieved from the same field with the crude oil and was used as a water-based fluid phase in this research.

Total dissolved solid (TDS) is the quantity of all organic and inorganic non-particulate material (Houston, 2007) and total suspended solid (TSS) qualities were determined based on the conventional procedure for examination of water and wastewater standardized by the the American Public Health Association (APHA) 2540-B, and 2540-C, respectively. American Petroleum Institute

Recommended Practice 45 (API RP-45) method is the recommended practice for analysis of oilfield waters (API, 1968), and X-ray fluorescence (XRF) spectrometers were used to quantify other substances contained in the FW (Jenkins, 1999). The FW properties are represented in Table 3.3.

Table 3.3. The properties of FW.

Properties	**Unit**	**Value**
TDS	mg/l	280
TSS	mg/l	200
SG*	-	1.0068
pH	-	7.065
Composition:		
- Cl^-	mg/l	24.21
- SO_4^{2-}	mg/l	790.08
- HCO_3^-	mg/l	135.45
- Na	mg/l	0.01
- Ca	mg/l	174.8
- Mg	mg/l	0.01
- Ba	mg/l	13.0
- K	mg/l	27.9
- Fe	mg/l	1.2

*SG = specific gravity

3.1.2.3 Nanofluids

Various concentrations of aluminosilicate NFs were arranged for this research. The aluminosilicate NFs were formulated using the two-step procedure. The first stage is to create NP by two basic strategies, such as top-down and bottom-up operations. The phrase 'top-down' denotes the mechanical destruction of origin substance utilize a crushing operation. In the 'bottom-up' approach, constructions are created by chemical operations. The assortment of any operations relies on the chemical configuration, and the chosen characteristics are detailed for NPs (Nanowerk, 2020). However, the synthesis of the aluminosilicate NPs is outside the purview of this research. The second stage is to disperse the aluminosilicate NPs powder into FW as a fluidic base in the next handling stage employing ultrasonic agitation (ultra-sonicator) for approximately 24 minutes for each concen-

Table 3.4. The properties of aluminosilicate NFs at room condition.

NFs	Concentration (ppm)	Density (g/cm^3)	Viscosity (cP)	pH
a	1	0.98913	0.7	7.06
b	10	0.98903	1.05	7.39
c	20	0.98897	1.15	8.85

Figure 3.1. Ultra-sonicator apparatus.

tration (Yu and Xie, 2012). This two-stage procedure is known as the cheapest technique to create NFs on significant numbers (Jafari et al., 2006). The ultra-sonic agitation apparatus are shown in Figure 3.1, and the aluminosilicate NFs properties are represented in Table 3.4.

3.1.3 Cores

As a reservoir rock representative, the Bentheimer sandstone (SS) core plugs were used in this research, which is universally applicable in examining liquid flow in porous media. SS is considered an ideal sedimentary rock for reservoir studies due to lateral continuity and similar block scale properties. Clarke et al. (2016) mentioned that the Bentheimer SS has a uniform texture with large grains, and the pore-throat distribution is well-characterized by a single peak.

In this research, the core diameter is 1 inch with 1 foot long and then cut into seven sections with an estimated length per core of 1.5 inches, represented in Figure 3.2. All core plugs were first purified employing toluene over a Soxhlet extraction equipment at 60–70 °C for approximately 12 hours and cleaned with methanol in similar circumstances, and the interval followed. The Bentheimer core plug properties are represented in Table 3.5.

Table 3.5. The properties of Bentheimer SS core plug.

Core	Diameter (cm)	Length (cm)	Porosity (%)	Permeability (mD)	S_{oi}* (%)
N1	2.545	3.486	19.97	316.93	84.69
N2	2.545	3.515	19.61	565.41	82.17
N8	2.545	3.525	20.37	633.76	82.40
N4	2.545	3.523	20.17	340.61	82.95
N5	2.545	3.543	19.74	374.65	82.04
N7	2.545	3.523	19.33	359.06	84.53

* Initial oil saturation

Figure 3.2. The Bentheimer SS core plugs.

3.2 Experimental methods

3.2.1 Stability investigation

Kissa (2017) stated that the NPs solution is defined as unchanging during the number of molecules in a component of the quantity that is tenacious over time. Healy (2006) opined that the constancy of silica solutions relies on the construction of its surfaces and is connected to aqueous particles that designated the adjacent area's appearances. Furthermore, Degabriel et al. (2018) declared that the form of the particles considerably influences nano-solution stability. Thus, the solution formed by spheres is more stable than those formed by the rods of the same diameter.

The existence of the silanol (Si-OH) assemblies on silica surfaces serves as an adhesive point for water. When an improvement in electroplate concentration filters the surface charge of NPs and decreases the energy barricade for agglomeration, it consequently drives to faster aggregation. The aggregation of silica-based NPs will occur because of the presence of electrolytes. Jenkins et al. (2008, 2007) revealed that the surface charge power of silica NP in the presence of sodium background affects the collection of water particles around the surface of silica and water-particle contact. This force is known as the oscillatory interparticle force. The NFs are unbalanced if the molecules agglomerate and generate a more significant secondary shape than the original molecule dimensions.

The visual stability of the sedimentation investigation was carried out over a specific duration, approximately ten days, and at different conditions of ambient temperature (25 °C) and reservoir temperature (60 °C). The three desired concentrations of nanofluids are placed into the tube (4-6 ml) and compared regarding the particle aggregation day-by-day capturing the image. A heating cabinet was used for observation at higher temperatures. This investigation was performed to know the behavior of NPs versus time.

3.2.2 Wettability index experiment

Wettability is defined as the capability of a liquid to keep connected with a solid surface. The adhesive and cohesive forces between solids and liquids determine wettability. Cohesive forces affect the same types of molecules. In liquids or solids, molecules are pulled towards one another because of cohesion between the molecules. Adhesion is the interaction between different molecules. The balance between these forces defines the degree of wettability. Wettability is essential in the connection or reliability of two substances. The Amott and Amott-Harvey methods are a popularly-used assessment quantity of core plug's wettability. According to Al-Anssari et al. (2017) the more significant substance of NP likely decreased nano-solution firmness and required the additive factor. Since additive factors might modify the system's wettability, identifying NPs concentration is performed, allowing the NFs can be preserved without adding the additive.

This research utilized the Amott-Harvey method to determine the wettability index (WI) (Figure 3.3). The Amott-Harvey method is established on the ordinary imbibition and charges the dislodgment of oil and water through porous media over time. This method is followed by the core flooding of the sample to achieve S_{or}, then imbibition of oil back into the core inside an oil-filled tube, and other core floods with oil. This process has no legitimacy as a definite determination. However, it is still standards-based for comparison of the wettability of several core plugs.

The Amott-Harvey method procedure is separated into two phases. The first phase is the saturated oil core plug was positioned in the imbibition chamber bounded by FW for a specified time frame. The oil in the core-pore is removed by water until stability is achieved; next, some produced oil is recorded. The centrifugal force controlled the obliged imbibition to accomplish S_{or}. Afterward, the procedure was replicated with an imbibition chamber and oil flooding apparatus. The process that occurs is that oil will captivate toward core plugs, and

Figure 3.3. Amott cell apparatus.

water and oil will be streamed simultaneously. Comparable to the prior procedure, water enduring into the core plug forced-out using the centrifugal force. Then, the disqualified water was assessed to measure the initial water saturation (S_{wi}). Post-registering amount of production in each phase, the Amott index, WI can be calculated using Equation (3.1).

$$WI = I_{w} - I_{o} \tag{3.1}$$

Where I_w is water imbibition index and defined as a ratio of natural saturation change to natural advantageous determined saturation change for water $\left(\frac{S_{pw}-S_{wi}}{1-S_{wi}-S_{or}}\right)$. I_o is the oil imbibition index and defined as a ratio of natural saturation change to natural advantageous determined saturation change for oil $\left(\frac{S_{po}-S_{or}}{1-S_{wi}-S_{or}}\right)$, with natural water saturation marked as S_{pw}, natural oil saturation marked as S_{po}, initial water saturation marked as S_{wi}, and residual oil saturation marked as S_{or}.

The water-wet core especially demonstrated a zero value for displacement with a water ratio and a positive displacement from the oil ratio. The WI value

result is positive, which is approaching plus one for a sample with a stronger water-wet. The oil-wet cores were showed the contrary, e.g., positive for water displacement ratio and zero for oil displacement ratio. Thus the resulting ratio is negative, advancing minus one for stronger oil-wet. An Amott index describes neutral wettability with a value near zero. The WI is given as a value between +1 and -1, where a water-wet system, lightly water-wet, neutral-wet, lightly oil-wet, and oil-wet has the value range from 1−0.3, 0.3−0.1, 0.1−-0.1, -0.1−-0.3 and -0.3−-1, respectively, and shown in Figure 3.4.

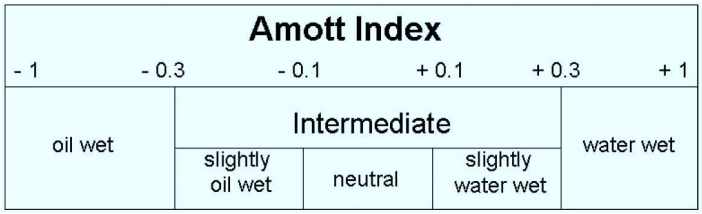

Figure 3.4. Amott-Harvey WI classification.

3.2.3 IFT measurement

IFT is a determination of unified or additional force existing at an edge ascending from the inequity of forces between molecules. Once two contrary phases connect one another, the particles at the edge contact an inequity force. The edge, as mentioned earlier, induced the collection of released force at the border. This released force is called surface released energy and is possibly calculated by measuring the ratio of energy per area or energy needed to enhance the active region of the edge over the number of units. Alternatively, to illustrate this kind of condition as holding border stress or IFT, equaling measured as an energy per distance determination. This surface released energy inclines to lessen the surface area, e.g., this explains why liquid droplets and air foams are circular. The surface free energy occurs in all types of interfaces. The measurement is usually attributed to the IFT if the surface examined is the interface between the insoluble fluids. The typical unit for IFT is dyne/cm or mN/m, and those units are equal.

The IFT between oil-NFs was estimated using a spinning drop method (TX-500C/D goniometer) related to fluid density difference. In this method, a droplet of oil is inserted into a vessel of the denser liquid. The equipment rotation was kept at 6,000 revolutions per minute (rpm), and the temperature was established at 60 °C. This measurement requires at least about 30 minutes in each data collection. Due to the centrifugal force near the wall cylinder, oil droplets will elongate along the rotation axis. When the surface strain and centrifugal force reached the equilibrium, this extension will stop. This value is attained at the equilibrium position, which is used to estimate the IFT of a specific liquid employing a proper correlation. The formula for measuring IFT corresponds to the Vonnegut equation given by Equation (3.2) (Vonnegut, 1942).

$$\sigma = \frac{\Delta\rho\omega^2}{4}.r^3 \tag{3.2}$$

where IFT is σ [dyne/cm]; density difference is $\Delta\rho$ [g/cm^3]; rotation angular velocity is ω [rotation/minute]; the interface effective radius is r [cm].

The spinning drop TX-500CD apparatus and an example of IFT measurement outcomes are represented in Figure 3.5 and Figure 3.6, respectively.

Figure 3.5. Spinning drop tensiometer instrument.

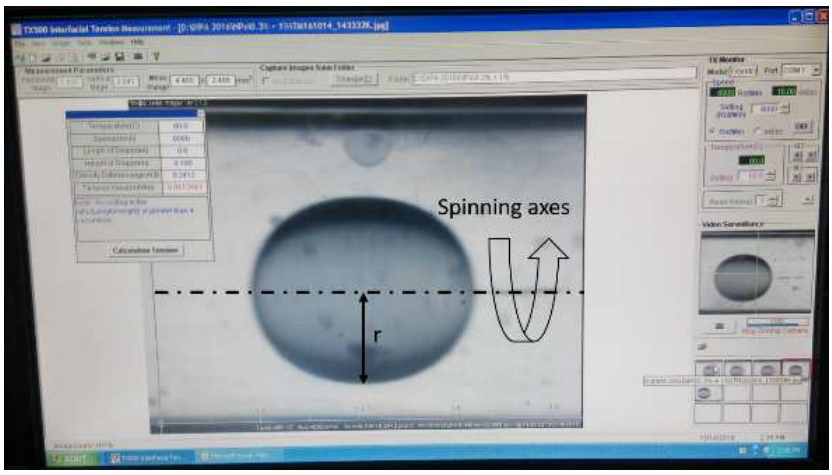

Figure 3.6. The illustration of IFT determination results in employing the spinning drop technique.

3.2.4 Core flooding experiment

The core flooding investigation is frequently used in oil and gas industries to examine liquid discharge in porous media, adsorption, and oil recovery at particular reservoir conditions. Core flood determination allows them to carry out several behaviors depending on the suitability, detailed application requirements, and existing interpretation approaches. Core flooding is usually achieved under consistent pressure differences across the core plug or consistent flow over the core plug. This consistent condition makes it easy to interpret the experimental data using a scientific model. Preserving a consistent pressure variance and stream circumstances in realistic assessment environments may be problematic, and it might not be achieved, although using high-quality equipment. Consequently, preferably using an interpretation method that can calculate variable flow conditions.

This experiment is commonly performed under controlled thermodynamic conditions and continuous core flood sequence (Mandal et al., 2010). Even though the core flooding experiment is complicated and time-consuming, it can still deliver the most suitable and dependable information for evaluating EOR systems. This research has utilized the Hassler core handle among Teledyne ISCO 1000D syringe pump and the equipment arrangement represented in Figure 3.7.

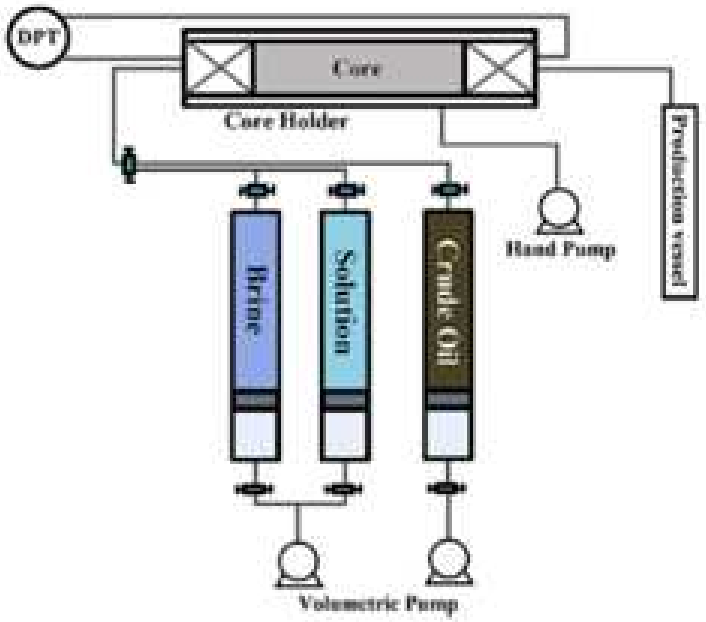

Figure 3.7. Diagram of core flooding experimental equipment.

NFs with various concentrations were equipped for displacement experiments. The two-component (oil-FW) core flooding apparatus arrangement was organized, and the Hassler compartment was positioned in a heat chamber. The displacement assessments were completed in subsequent flooding and conducted at reservoir temperature (60 °C). Throughout the procedure, the confining pressure and injection value were kept at 100 psig and 0.2 cm^3/min, respectively. These values scheme was adopted to imitate the regular liquid rates in the conditions common reservoir. These assessments were performed for all concentrations of NFs with a similar scenario.

3.3 Results and discussions

3.3.1 Stability analysis

The DLVO concept is the most appropriate method to characterize the mechanism of the constancy of solutions. This concept mainly addresses the stability between two different forces, which are attractive and repulsive. It also clarifies the ten-

dency of solutions to agglomerate or to remain separated. The van der Waals' attraction and repulsion describe how particular colloidal structures agglomerate, whereas others remain separated and dissolved in solution (Yousefvand and Jafari, 2018). The stability of the colloids is expressed by the combination of attraction and repulsion force (Hamaker, 1937). The energy barrier would appear if there was a repulsive section that reached the maximum repulsive energy. The bigger the barricade is, the more the system will be stable (Rao, 2010). Another influence in monitoring constancy is the ionic force, which performs similarly to electrolyte concentration (Saleh et al., 2008).

In the previous investigation by Kuang et al. (2018), that silicon dioxide (SiO_2) NFs were stable, while alumina (Al_2O_3) NFs will be stable when the stabilizer agent was added to its suspension. Yu and Xie (2012) described the agglomeration of NPs made blockage of pore throats of rocks and reduced the heat-conducting element. Therefore, the arrangement of NFs stabilization is a substantial problem (Das et al., 2007).

The stability of NFs was investigated by observing the aluminosilicate NPs suspension samples. The stability was detected by visual examination during a particular time at several temperatures (25 °C and 60 °C). The 1, 10, and 20 ppm of NPs were added after initiating the test without NPs. The results of visual observation at 25 °C and 60 °C can be observed in Figure 3.8.

Based on the test results, the accumulation of aluminosilicate NPs kept NFs constant with no visible agglomeration even at the reservoir temperature. These results follow the recent investigation by Hu et al. (2016). Moreover, rendering to the DLVO concept, particle stability in suspension is determined by the amount of attractive and repulsive electrostatic force stated by van der Waals triggered by electric double layer contact due to Brownian impact. The suspension will not be stable if the repulsive force is more insignificant than the attractive force, then the elements will agglomerate. Emphasize that 20 ppm NFs at reservoir temperatures is slightly dense, while it could not be viewed clearly in Figure 3.8.

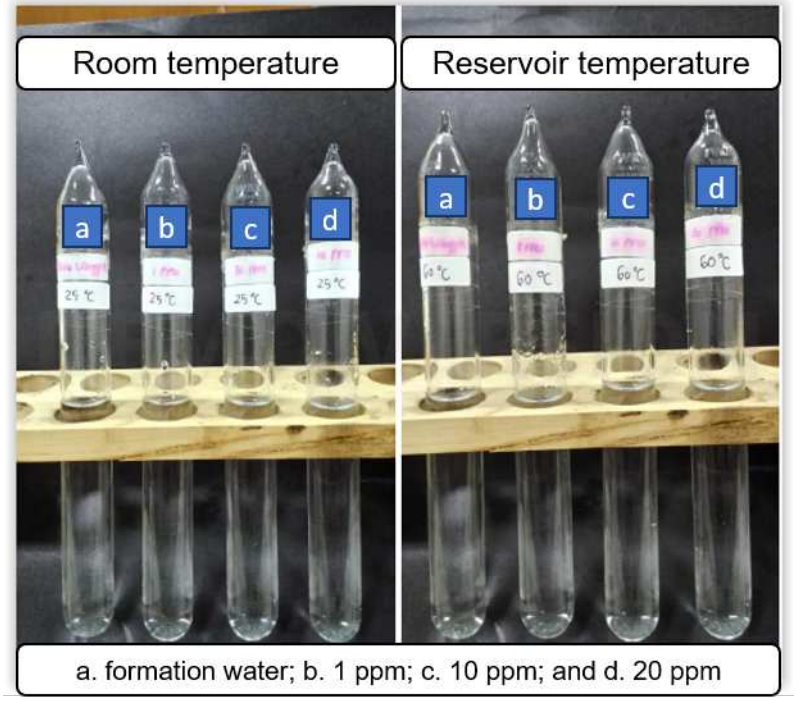

Figure 3.8. Observation of visual stability at different temperatures with varying NPs concentrations.

The agglomeration might occur because of the alumina content in aluminosilicate NPs.

3.3.2 Wettability index determination

The Amott-Harvey imbibition assessment is a frequently used determination to quantity the wettability of cores. Amott (1959) concluded that altering the wettability of essential reservoir aspects raised oil recovery. Giraldo et al. (2013) opined that the efficiency of NPs as a wettability modification would be improved with the concentration of NFs lower than or equal to 500 ppm. By altering wettability, the residual oil saturation will decrease, and the oil phase flow will be improved.

During the imbibition procedure, there was no substantial increase in oil produced from day one of observation at 30-minute intervals. Nevertheless, oil recovery was significant on the first day, while in the following days, the increase was low. For NFs, the response was low if compared with FW. Observing the

imbibition for seven days, the recovery from the NFs did not provide a significant result compared to recovery using FW. In macroscopic observations, the NFs tend to hold oil out, and it happened that the oil grain that came out looks more prominent than the oil grain using FW. If the NFs works well, the solution should be able to break the droplet that will come out of the core with a smaller size so that oil can easily come out of the core pores and be lost from the cores. Even so, the highest oil recovery starts from 10 ppm, 1 ppm, 20 ppm, and FW, respectively. The core plugs treated with NFs had a low or slower spontaneous imbibition rate, which might occur due to permeability impairment during NFs injection and drying process.

The WI values are calculated based on Equation (3.1) and presented the results in Table 3.6. While revealed in Table 3.6, the core plugs tested with several solutions, including NFs, proposed the WI of a water-wet arrangement, in which the 10 ppm NFs the core sample showed the strongest water-wet system. The outcomes indicated that the aluminosilicate NPs are readily adsorbed to the surface concealed by the oil phase and provide the durability of the treatment. The NFs were absorbed on rock surfaces, altering the wettability by oxidizing crude oil removed by ion pairs. This result agrees for this purpose by Li and Torsæter (2014); Hendraningrat and Torsæter (2014); Giraldo et al. (2013).

Table 3.6. The influence of NPs on the WI.

Core ID	Concentration (ppm)	Saturation				Amott Test			
		S_{oi}	S_{pw}	S_{or}	S_{po}	I_w	I_o	WI	Remark
N1	0	0.15	0.59	0.38	0.38	0.94	0.03	0.91	water-wet
N2	1	0.17	0.70	0.29	0.29	0.99	0.01	0.98	water-wet
N8	10	0.16	0.67	0.32	0.32	1.00	0.01	0.99	water-wet
N4	20	0.17	0.67	0.32	0.32	0.99	0.01	0.98	water-wet

3.3.3 IFT determination

IFT of water will be reduced by attracting adsorption at the liquid-air interface when surfactants or chemicals are mixed with water. Therefore finally decreas-

ing the suspension surface free energy. Consequently, the monomeric chemical concentration becomes adsorbed at the air-water edge, therefore reducing the IFT turn into nearly constant. The concentration equivalent to the lowest IFT is called critical micelle concentration (CMC). Any other improvement in the chemical concentration beyond this boundary will lead to the reform of micelles with a constant IFT or a slight improvement in IFT (Mandal and Bera, 2012). The IFT measured between the oil and FW, utilized the spinning drop method. The IFT values are calculated based on Equation (3.2), and the result was 20.67 dyne/cm at 60 °C. The presence of 1, 10, and 20 ppm of aluminosilicate NPs decreased the IFT from 20.67 to 9.09, 5.96, and 6.92 dyne/cm, respectively, and the results are shown in Table 3.7. Compared with single conventional chemical flooding or surfactant, the lowest oil-water IFT by a particular surfactant could reach 10^{-3} to 10^{-2} dyne/cm. Even though NFs cannot achieve those values, if NPs are modified with hydrophilic groups will create a Janus particle, then the particle possesses the ability to decrease IFT significantly (Peng et al., 2017).

Particular IFT measurement results amongst the oil and liquid reduced about 30-40% due to the addition of NPs (Figure 3.9), which might indicate that the higher is the NFs concentration, the lesser IFT value can be accomplished when the NFs is in the stable condition. This result complied with Parvazdavani et al. (2014), Li et al. (2013) and Hendraningrat et al. (2013c).

Table 3.7. The effect of NPs on IFT.

Aluminosilicate NFs	**IFT (dyne/cm)**
0 ppm (FW)	20.67
1 ppm	9.09
10 ppm	5.96
20 ppm	6.92

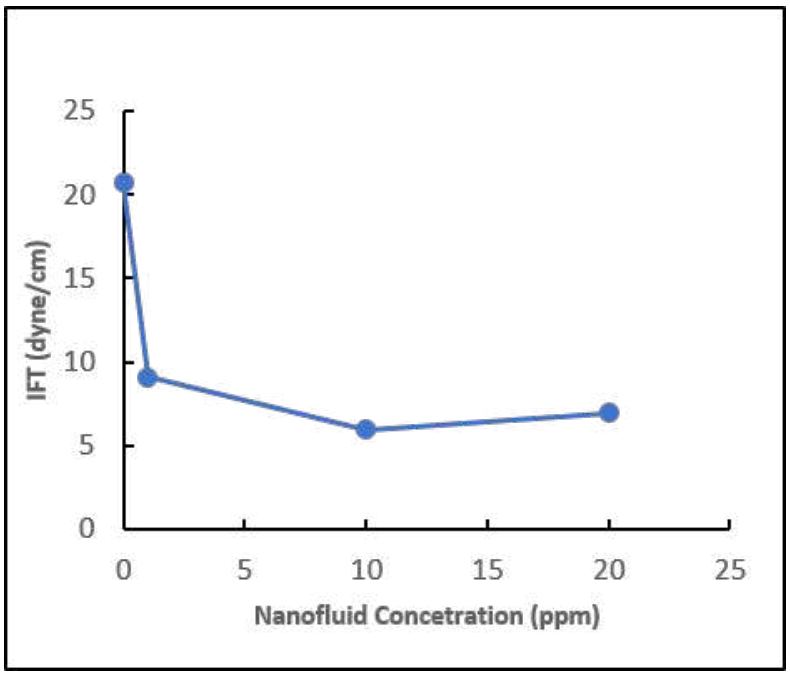

Figure 3.9. The IFT measurement at various concentrations.

3.3.4 Core flooding experiment

Various concentrations of NFs were designed for core flooding experiments. The Hassler core chamber remained positioned in a heat chamber. These experiments were conducted at 60°C. Through a particular procedure, the ambient pressure and injection were kept at 100 psig and 0.2 cm^3/min, respectively. The core flooding experiments were carried out for all schemes of NFs by identical setting, which is the nano flooding treated as tertiary recovery.

Through the first stage, the forced imbibition procedure, the FW was injected continuously until the S_{or} achieved, termed as conventional water flooding (WF) method or secondary recovery process (Howard et al., 1990). Anderson (1987) concluded that in the WF's procedure, water was consistently transferred over a porous media and held a tendency to be absorbed toward minor or middle-sized pores. Oil dislocates water into larger pores, and after secondary recovery, almost all of the remaining oil is separated and immobile. The NFs was injected in the following stage as a nano flooding method or tertiary recovery process. When they were added into the core plug, the aluminosilicate NFs engaged with the im-

mobile oil then mobilized them. The discharged oil from a core was documented and also assessed in a tube collector through the procedure.

Figure 3.10a illustrated that FW was injected into the core plug, approximately by 5.2 (PV). When no more oil was formed, then it continued to inject 1 ppm of NFs (approximately 5.4 PV). The final oil saturation can be established at the tertiary recovery. As shown in Figure 3.10b and Figure 3.10c, to achieved the S_{or} stage, the FW was injected by 5.2 and 5.6 PV, respectively, and for the final stage, the injecting of 10 and 20 ppm of NFs was required of 5.5 and 4.6 PV, respectively. The incremental of oil recovery was observed when nano flooding (Nano-F) was conducted with three concentrations of NFs. Oil recovery after WF with 1, 10, and 20 ppm of NFs was 54.79%, 56.95%, and 49.59%, respectively. While oil recovery after nano flooding was 61.64%, 72.54%, and 54.03%, respectively. The detailed summary of the core flooding experiments are shown in Table 3.8.

Table 3.8. Summarized core flooding experiments.

NFs	Core ID	Oil recovery (%-IOIP)			S_{or} (%-PV)	
		WF	Nano-F	Total	WF	Nano-F
1 ppm	N5	54.79	6.85	61.64	37.1	31.48
10 ppm	N5	56.95	15.59	72.54	35.66	22.75
20 ppm	N7	49.59	4.44	54.03	42.64	38.88

The research revealed that the injection of NFs remarkably affects the additional oil recovery. It is suspected the additional oil recovery would be developed with an escalation in NPs concentrations, as described in previous studies by Hendraningrat et al. (2013d) and Joonaki and Ghanaatian (2014). Nevertheless, the most significant incremental oil recovery was accomplished at 10 ppm NFs. The additional oil recovery by 20 ppm is lesser than the 10 ppm NFs. This phenomenon happened from the agglomeration of the NPs. This determination result was consistent with (Hendraningrat et al., 2013a). Hence, it is highly suggested to determine the CMC earlier.

Even though the NFs are stable at reservoir temperature, the 20 ppm NFs

might slightly agglomerate, revealing the cloudy condition. They altered the wettability of the cores turning to stronger water-wet and decreasing the IFT. The consequences of the NPs individual bond on the liquid-liquid and solid-liquid connections result in the wettability alteration and IFT reduction. The structural disjoining pressure improved with the NPs existence, which formed an attractive electrostatic force to the core surface. Since this pressure is the primary dominant mechanism tempted by NPs, it greatly affected the recovery of additional oil in these core flood tests.

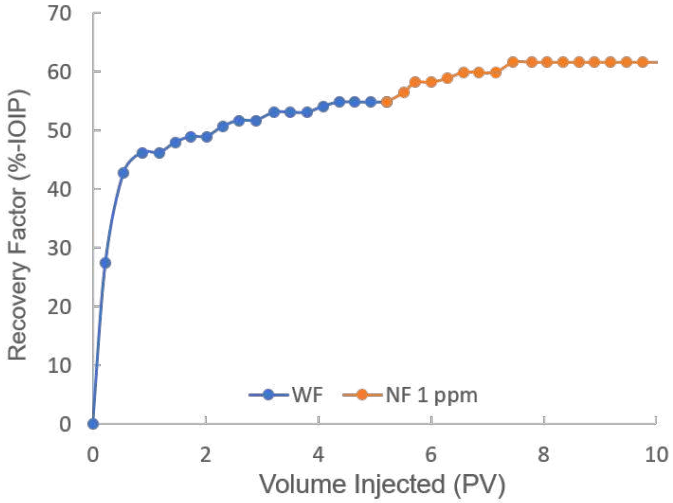

(a) 1 ppm of aluminosilicate NPs

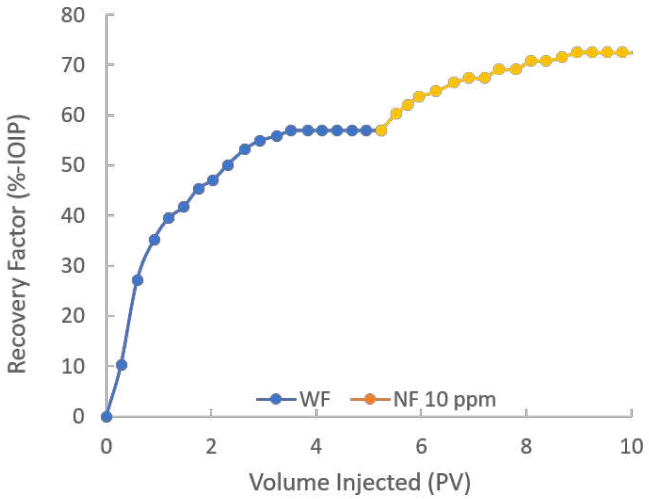

(b) 10 ppm of aluminosilicate NPs

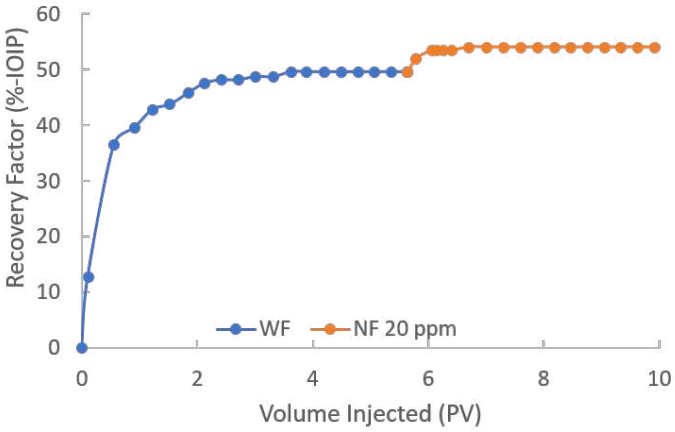

(c) 20 ppm of aluminosilicate NPs

Figure 3.10. The induce of NFs injection on additional oil recovery.

Chapter 4

Snowtex® ST-AK nanofluids as an EOR agent

This chapter explains the methodology and procedure applied in all the experiments conducted with Snowtex® ST-AK NFs, which covers IFT determination, wettability alteration measurements employing the contact angle method as well as displacement tests. This chapter presents the second of a series of a publication titled *Application of Functionalized Cationic-Acidic Silica-Alumina-Based NFs for Enhanced Oil Recovery*.

4.1 Materials

4.1.1 Synthetic brine

Brine is defined as a salt suspension, and it is the high concentration of sodium chloride in an aqueous solution (Wikipedia, 2020). While Houston (2007) reported that in the representative brine or sea-water composition analyses performed on solutions obtained from sedimentary basins around the world, the major salt components contained are Na^+, K^+, Ca^{2+}, Mg^{2+}, Cl^-, HCO_3^-, and SO_4^{2-}, with TDS from 100 to 300,000 ppm. Synthetic brine (SB) is defined as a mixture of

dissolved mineral salts that simulates sea-water. From a scientific perspective, the SB has a reproducibility advantage over natural sea-water because it is fixed to a standard-defined formula. The SB prepared for the experiments was to represent the average salinity of sea-water and was used as the water-based fluid phase to perform this research. The SB, expressed as reservoir IFT, was prepared from sodium chloride (NaCl) with a concentration of 3.0 wt% (approximately 30,000 ppm) with distilled water as base fluid suspension. This salinity was chosen from a typically defined sea-water concentration (Wikipedia, 2020). The density of this suspension at laboratory temperature (25 °C) is 1.006 g/cm^3.

4.1.2 Nanofluids

Snowtex® ST-AK (denoted as ST-AK) NFs with an average particle size is 12 nm were provided from Nissan Chemical Co., Ltd, Japan. The ST-AK NFs are cationic-acidic silica-alumina-based, silicon dioxide (SiO_2) and alumina (Al_2O_3) content not more than 20 and 2.5 wt%, respectively. As mentioned in the previous chapter (section 3.1.2.3), there are two methods for synthesize NFs. The bottom-up method was used to synthesized the ST-AK NFs. the ST-AK NFs were made by employing a chemical process from the raw material of sodium silicate under particular conditions, so that produced stable and homogeneous NFs. However, the synthesis of these NFs is beyond scope of this research. The NFs were prepared in six concentration batches and were formulated by homogenizing NFs in distilled water using a conventional agitator for approximately ten minutes for each concentration (Rao, 2010). The ST-AK NFs properties are presented in Table 4.1.

Table 4.1. The properties of ST-AK NFs.

Properties	Unit	Measure*
Particle size	nm	12
Appearance	-	Clear collagen
SG (@20 °C)	-	1.144
pH (@20 °C)	-	4.6
μ** (@20 °C)	cP	3.8
SiO_2 content	wt-%	17.7
Al_2O_3 content	wt-%	2.1

*provided by Nissan Chemical Co., Ltd.
**Viscosity

4.1.3 Synthetic oil

Synthetic oil is made artificially and consists of various chemical compounds and alkane hydrocarbons, and is also used as a substitute for oil-refined. The synthetic oil used in this research is n-decane, known as a non-polar solvent, insoluble in water, and flammable. Moreover, its vapor may be narcotic in high concentrations. These chemical compounds are straight-chain alkane with ten carbon atoms and form a colorless liquid, found in ordinary organic and an alkane hydrocarbon mixture, with a chemical formula of $CH_3(CH_2)_8CH_3$ or $C_{10}H_{22}$ and result in a compound mixture of carbon chains. Furthermore, n-decane represents a constituent of the paraffin fraction of crude oil and natural gas. N-decane is released to the environment via the manufacture, use, and disposal of many products associated with the petroleum and gasoline industries (Howard et al., 1990). The density of n-decane is 0.73 g/cm^3 at 20 °C.

4.1.4 Porous media

The SS is recognized as a clastic sedimentary rock consisting mainly of grains of rock or sand-sized minerals (quartz sand). Thus, sometimes it bears silt and clay, also contain significant quantities of feldspar. Developing a comprehensive understanding of the various properties of SS is essential in determining fluid-rock interactions. The petroleum industry uses various types of SS for traditional

porous media in laboratory experiments. The data obtained from these tests can be compared with similar experimental data carried out using reservoir cores. Three of the most widely used standard rock are Baker dolomite, Berea SS, and Bentheimer SS.

The solid substrate used to determine wettability behavior with silica-alumina-based NFs is the Berea SS core plug. This SS is considered as water-wet and was used as porous media in this research (Hendraningrat, 2015; Hendraningrat et al., 2013c). Potts and Kuehne (1988) stated benefits of using a Berea SS in a displacement test experiment included a uniform rock property, being commercially available, and inexpensive. The Berea SS properties are presented in Table 4.2.

Table 4.2. Properties of Berea SS core plug.

Core	Diameter (cm)	Length (cm)	Porosity (%)	Permeability (mD)
C-1	2.52	3.61	22.29	529.316
C-2	2.52	3.39	20.93	564.650
C-4	2.52	3.47	20.99	505.810
C-5	2.52	3.54	22.31	565.362
C-6	2.52	3.41	18.04	519.030
SP-6	2.51	3.32	17.53	529.122

4.2 Experimental methods

4.2.1 IFT measurements

Green and Willhite (1998) reported that the effectiveness of process fluids in removing oil from the rocks at the microscopic scale is a significant aspect of each EOR process. IFT is the force that restrains the surface of the specific phases together and must be examined to determine its significance in oil recovery. Several methods for measuring the IFT have been discussed in Chapter 2, section 2.3.3. The spinning drop method is commonly used to measure the IFT (Chung

et al., 2018; Jia et al., 2017; Fuseni et al., 2013; Gao and Sharma, 2013). In this research, the IFT measurement adopted the spinning drop method to quantify the value between synthetic oil and NFs, and the procedure for this method has been discussed in Chapter 3, section 3.2.3.

4.2.2 Wettability alteration measurement

Liquid dispersions in porous media are influenced not only by forces at liquid-liquid interfaces but also by forces at liquid-solid interfaces. Wettability is a tendency of a liquid to spread on (Green and Willhite, 1998). When two immiscible liquids are placed in contact with a solid surface, one part of the liquids is usually attracted to the surface more strongly than the other. In accords with Morrow (1990), the decrease in water wetness has an impact that the oil recovery will be decreasing as well. Therefore, wettability has an essential role in oil recovery. The contact angle method is widely used to specify the wettability alteration (Jiang et al., 2017; Idogun et al., 2016; Li and Torsæter, 2014; Chaudhury, 2003; Anderson, 1987).

The drop shape analysis is commonly used in determining the contact angle. The contact angle is determined by image analysis of the angle between the calculated droplet shape function and the sample surface. When conducting a measurement, the scale of the video images is measured in advance to provide access to the actual decrease in dimensions. The schematic diagram of the drop shape analysis is shown in Figure 4.1

The contact angle was measured directly on a Berea SS thin section employing the Attension Theta tensiometer. This system functions as a transient analyzer, which means it continuously captures images and can recall any image after a trigger event commences. Various dynamic events can complement the trigger. One such trigger is a real-time software detection of a decrease from the expenditure edge. The drop shape apparatus and an example of contact angle determination result are shown in Figures 4.2 and 4.3, respectively.

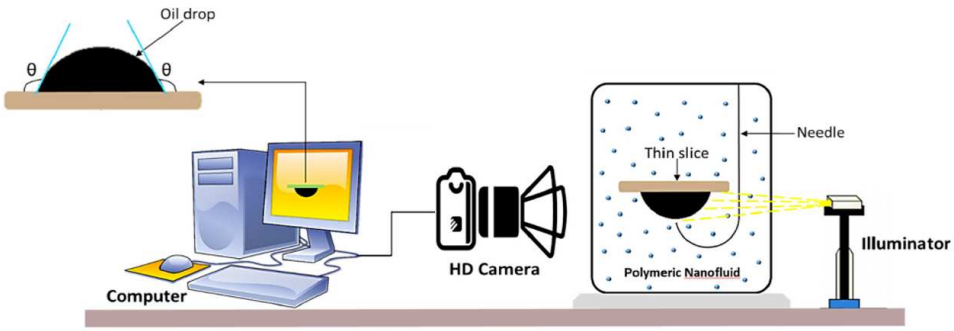

Figure 4.1. The schematic diagram of the three-phase drop shape analysis (illustrated by Ali et al. (2019)).

Figure 4.2. The Attension Theta is a drop shape analysis equipment.

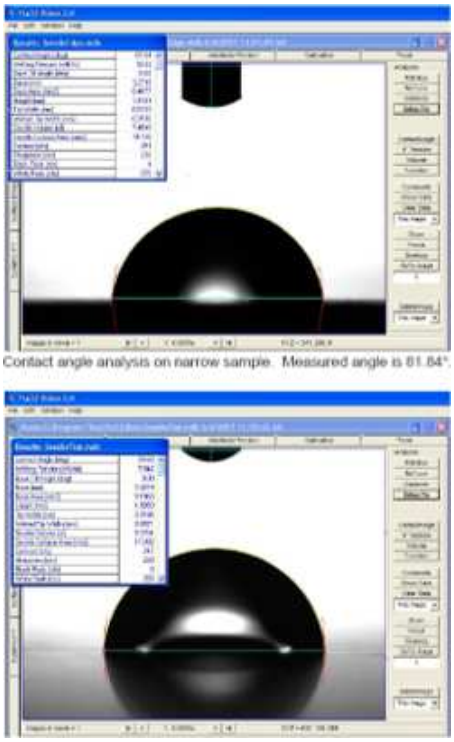

Figure 4.3. An example of contact angle measurement results.

4.2.3 Displacement test

The core flooding experiment is a displacement test commonly applied in the petroleum industry to investigate the adsorption at reservoir conditions, liquid discharge in a porous media, and oil recovery. The experiment can be carried out in various techniques depending on the convenience and specific application requirements and availability of the interpretation methods, which generally are performed under controlled thermodynamic conditions and using a continuous core flood sequence (Mandal et al., 2010). The schematic layout of the core flooding test setup can be viewed in Figure 4.4. This research employed the Hassler core holder with Teledyne ISCO 1000D syringe pump and Berea SS as the porous media. This test was proposed to acknowledge the capability of ST-AK NFs to improve residual oil in Berea SS core plugs after WF stage.

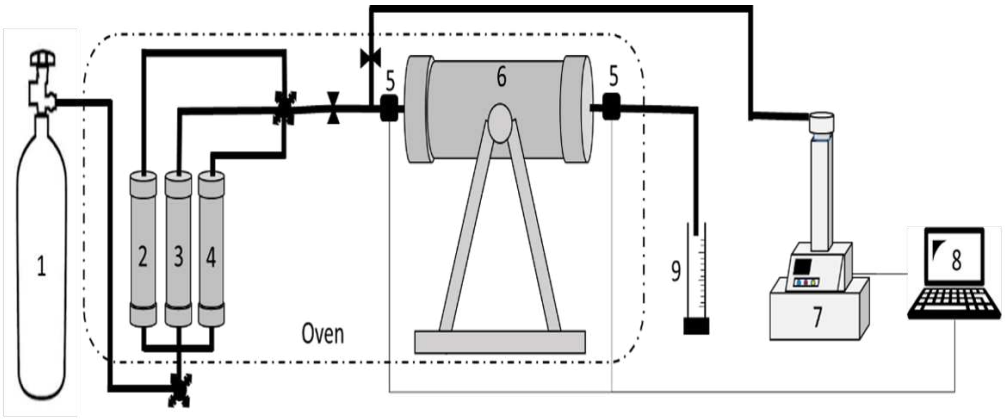

Figure caption: 1) Pump fluid; 2-4) Oil, brine, and NFs vessels, respectively; 5) Pressure transducer; 6) Core holder; 7) Isco pump; 8) Data gathering (computer); 9) Liquid collector.

Figure 4.4. Schematic design of core flooding experimental apparatus.

The various concentrations of NFs were prepared for this test and the tests were performed at a typical reservoir temperature (60 °C). The core-plug samples were saturated using SB, the confining pressure was maintained at 200 psig, and the injection rate was set at 0.3 cm^3/min. The injection rate was decided to mimic regular fluid velocities in a reservoir. Then the core was saturated with oil continuously. The water cut was less than 1 %, and the system was aged for three days

to simulate the reservoir equilibrium condition. Smith and Cobb (1997), Slathiel (1973), Schmid (1964), and Wissmann (1963) suggested that the wettability could be changed within three days. The WF stage was initiated until a single-phase brine was produced. Then, the ST-AK NFs were injected into the core as the tertiary recovery process. When NFs were injected into the core, the ST-AK NFs associated with the immobile oil and assembled the oil. Consecutively, SB was injected as post-flush WF to examine if additional oil could be extracted. Finally, the extracted oil from the core is gathered and measured in a two-phase liquid receiver. These tests were carried out for all the concentrations of NFs with the same experimental methodology.

4.3 Results and discussion

4.3.1 Effect of NFs on IFT

Throughout this experiment, the spinning drop method was used to quantify the IFT value between n-decane and NFs. This method explanation was already discussed in Chapter 3, section 3.2.3.

The IFT between n-decane and ST-AK NFs was measured at 60 °C. This condition was chosen based on previous work referenced (Wijayanto et al., 2019). The result of IFT measurements for SB is 14.91 dyne/cm, whereas for the concentration 0.0005, 0.0025, 0.005, 0.01, 0.1, and 0.5 wt-%, they are 4.59, 10.66, 17.15, 17.26, 15.68 and 15.88 dyne/cm, respectively, and is presented in Table 4.3.

The presence of NFs caused an increase in IFT, although in contrast, at very small concentrations at 0.0005 and 0.0025 wt%, the IFT value decreases. This result can be observed in Figure 4.5. According to Kuang et al. (2018), the increasing value of IFT occurred due to the absence of an attractive electrostatic force. This result was consistent with the previous works and studies by Sagala

Table 4.3. The effect of ST-AK NFs on IFT.

Sample	IFT (dyne/cm)
SB	14.91
0.0005 wt%	4.59
0.0025 wt%	10.66
0.005 wt%	17.15
0.01 wt%	17.26
0.1 wt%	15.68
0.5 wt%	15.88

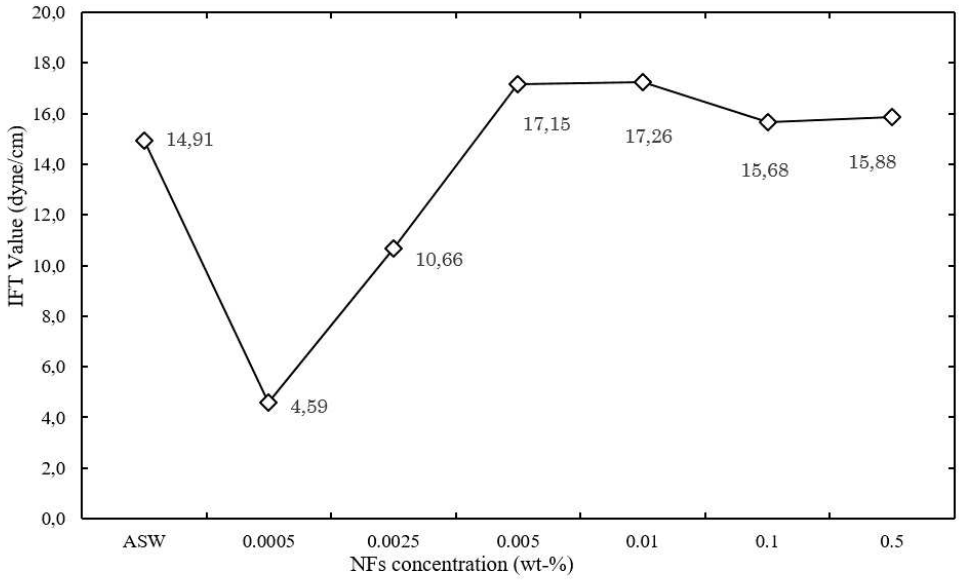

Figure 4.5. The IFT measurement at various concentrations.

et al. (2020); Wijayanto et al. (2019); Metin et al. (2012); Vignati et al. (2003), which suggests that the IFT decreases at a low concentration of NFs and increase after reaching the optimal concentration. However, the decrease or increase is tiny compared to the effect of decreasing IFT using surfactants as discussed by Betancur et al. (2019). The IFT reduction from their study was 0.0045, 0.0014, 0.00022 dyne/cm for surfactant with mass fraction of 0.15, 0.18, and 0.2 wt%, respectively. As Sagala et al. (2020) stated, the IFT reduction does not appear to be the dominant mechanism for recovering immobile oil using ST-AK NFs. From the standpoint of recovering immobile oil, NFs may have some effects on IFT reduction, but these effects are not significant. Furthermore, it is considered

that the IFT increases with an increase in the NFs concentration exceeding the optimum concentration due presumably to the agglomeration formation, which reduces the dispersity of NPs at the oil-water interface.

4.3.2 Effect of NFs on wettability alteration

The contact angle measurements were conducted based on image analysis derived from the software provided by the optical Attension Theta tensiometer. The SB content presents a significant role in determining the wettability of the rock, considering there are separated ionic species that will be attracted to ions of opposing forces on the rock and might endure adsorption. When the NFs were added to the SB, they reduce the contact angle. The results of contact angle measurements are summarized in Table 4.4.

The contact angle was reduced from 17.37° with SB only to 16.17° for the concentration of 0.0005 wt-% ST-AK NFs. The concentration of 0.0025, 0.005, and 0.01 wt-% ST-AK NFs, also reduced the contact angle from 17.37° to 8.40°, 12.76°, and 13.66°, respectively. However, in contrast, the contact angle determination for 0.1 and 0.5 wt-% ST-AK NFs increased from 17.37° to 17.57° and 28.82°, respectively.

Table 4.4. The effect of ST-AK NFs on wettability alteration.

Sample	Contact Angle (°)
SB	17.37
0.0005 wt%	16.17
0.0025 wt%	8.40
0.005 wt%	12.46
0.01 wt%	13.66
0.1 wt%	17.57
0.5 wt%	28.82

The reduced value of contact angle is due to the NFs adsorbed onto the rock surfaces. Since silica-alumina has diamagnetic properties, it alters the wettability to more water-wet by oil oxidization and provides the cationic charge to the particle surface (Yekeen et al., 2020; Ko et al., 2017; Hendraningrat et al., 2013a).

According to Liu et al. (2020), the cations could form the cation 'bridges' between surfaces and molecules. This 'bridge' is formed by electrolytes that bind two different NPs. This result is in line with the previous work by Wijayanto et al. (2019) and Dehaghani and Daneshfar (2019), which had shown the contact angle decreased to a particular NFs concentration and started to rise as it exceeded the optimum concentration (Figure 4.6). Below the optimum concentration, the contact angle decreases as the concentration of NPs increases. Suppose the NPs concentration exceeds optimum condition due to the cation bridging, several NPs are bounded, resulting in the collapse of the water film and increased contact angle (Xie et al., 2020). Similar findings were also reported by Dehaghani and Daneshfar (2019) and Hendraningrat (2015). Moreover, they opined that the changes in wettability are influenced by adsorption and structural disjoining pressure of the mechanism behind the discovered phenomenon. Alnarabiji and Husein (2020) also stated that the wettability alteration occurred through the structural disjoining pressure.

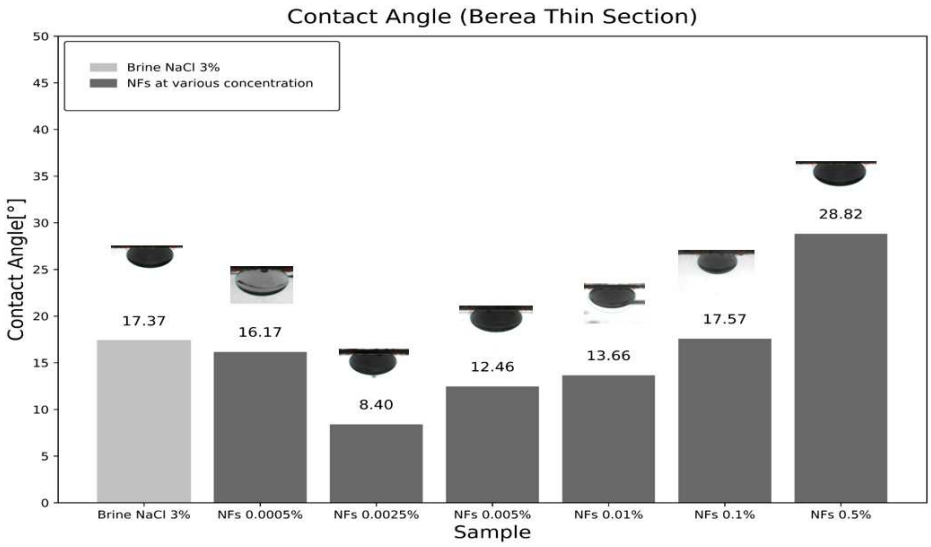

Figure 4.6. The effect of NFs on wettability alteration

4.3.3 Fluid displacement tests

The core flooding experiment is a displacement test popularly applied in the oil and gas industry to examine the fluids' discharge in a porous media, the adsorption at particular conditions, and the oil recovery. The oil recovery performances for WF and nano flooding (Nano-F), as well as the differential pressure profile, which can be observed in Figures 4.7 to 4.12. The average oil recovery is in the range of 22–40 % of OOIP and the S_{or} ranges from 31 to 37 % of the PV were obtained at the WF stage. As Morrow (1990) reported, the variations in oil recovery were caused by the complexity of the oil-brine-rock interactions. The NFs were injected as a tertiary recovery process (Nano-F) when a 100% water cut was achieved. The NFs successfully reduced the S_{or} and increased oil recovery. The summary of the core flooding experiment results can be viewed in Table 4.5.

Table 4.5. Summary of the displacement test experiments.

NFs (wt%)	Core ID	Oil recovery (%-OOIP)			S_{or} (%-PV)	
		WF	Nano-F	Total	WF	Nano-F
0.0005	SP-6	22.40	3.20	25.60	33.68	32.29
0.0025	C-6	36.36	9.09	45.45	34.20	29.32
0.005	C-5	37.50	5.00	42.50	31.73	29.19
0.01	C-1	40.00	4.76	44.76	31.13	28.64
0.1	C-2	34.00	2.50	36.50	37.28	35.87
0.5	C-4	35.00	0	35.00	35.78	35.78

Figures 4.7, 4.8, and 4.9 show that differential pressure started to rise as NFs were injected into the core. This increase may indicate the creation of a new oil bank in the Nano-F stage, which provides resistance to fluid movement. As the oil started producing, the differential pressure declined and eventually leveled off until no additional oil could be recovered. A similar response was observed when the post-flushing WF stage was initiated. However, the increase in differential pressure does not correspond to the increase in oil recovery.

A more pronounced differential pressure increase occurred with the higher NFs concentration, which can be observed in Figures 4.10 and 4.11. This phenomenon occurred due possibly to pore network blockage. Meanwhile, Figure 4.12 for the NFs concentration of 0.5 wt%, there was no incremental oil recovery as NFs were injected into the core, while the differential pressure gradually increased to the end of the injection. When the post-flush WF stage started, the differential pressure continued to increase without any incremental oil recovery. It may suggest that the effect of pores throat blockage was severe at higher concentrations.

These tests revealed that the addition of low concentration NFs affects the additional oil recovery. The dynamic fluid-rock interaction is more complicated than observed in the static fluid-rock interaction during the wettability determination and fluid-fluid interaction during the IFT measurement. The NFs were adsorbed at the rock pore surface without blocking the pore throats at low concentrations. It may be suggested that NFs did not agglomerate and were the most effective in recovering oil at an optimum concentration of 0.0025 wt%. At a higher concentration of 0.01 to 0.5 wt%, the adsorbed NFs harmed the core permeability reduction as indicated by the rising differential pressure.

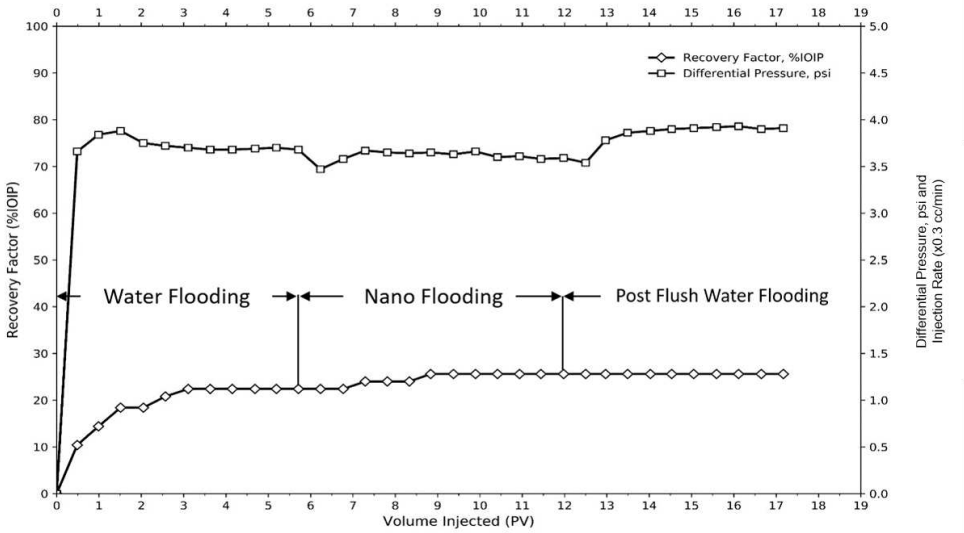

Figure 4.7. The core flooding test result of 0.0005 wt% ST-AK NFs

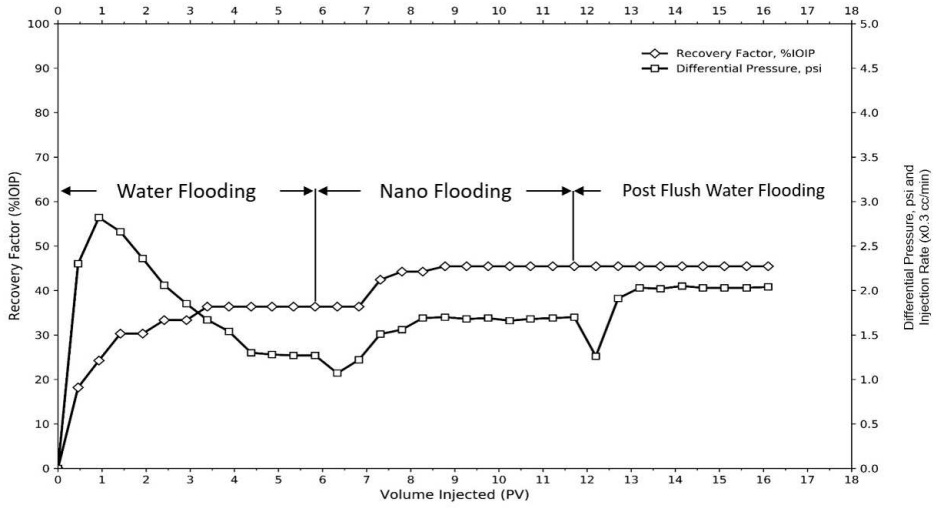

Figure 4.8. The core flooding test result of 0.0025 wt% ST-AK NFs

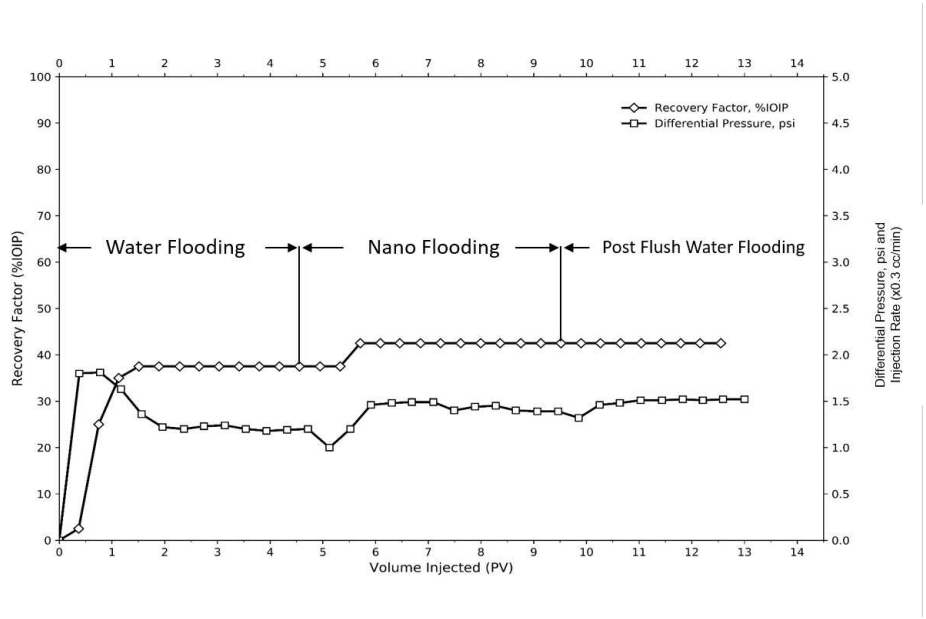

Figure 4.9. The core flooding test result of 0.005 wt% ST-AK NFs

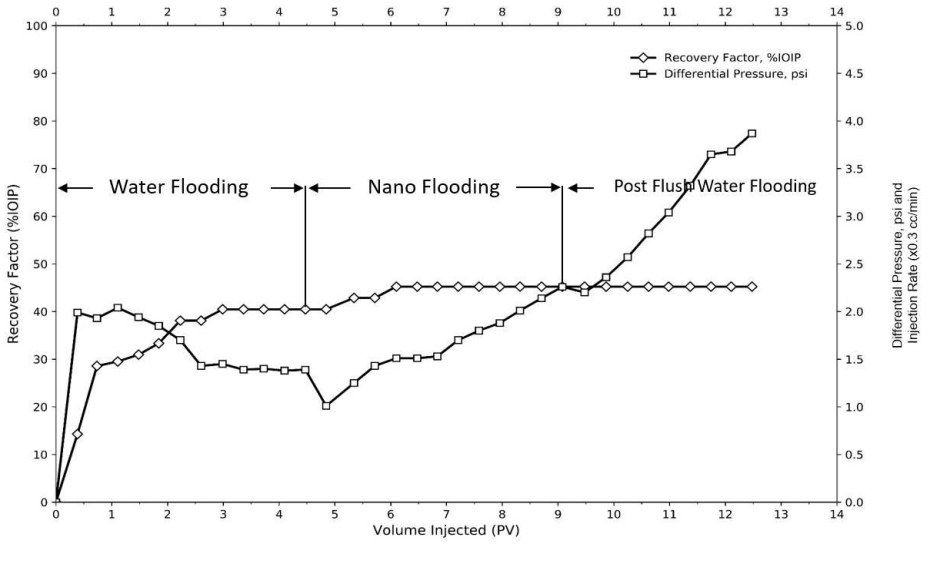

Figure 4.10. The core flooding test result of 0.01 wt% ST-AK NFs

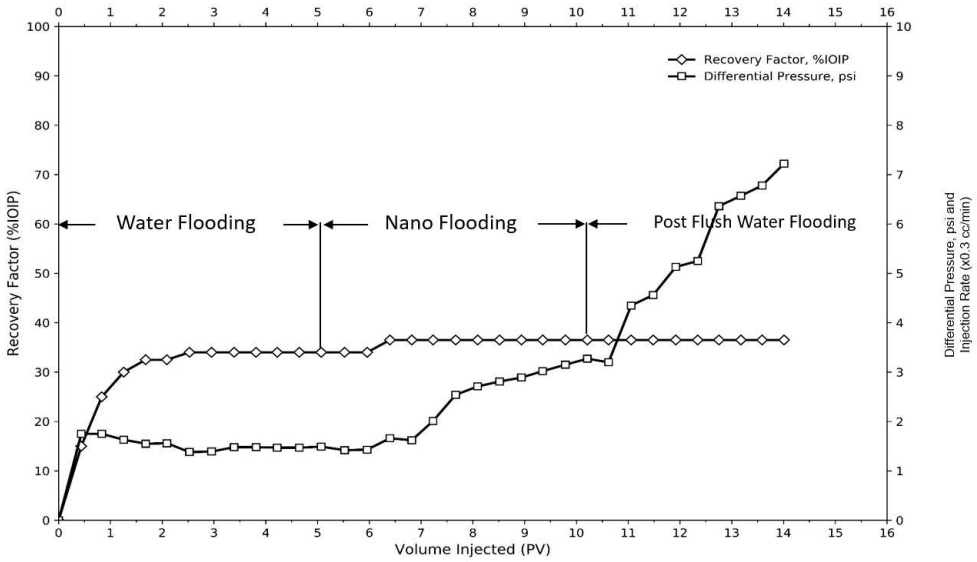

Figure 4.11. The core flooding test result of 0.1 wt% ST-AK NFs

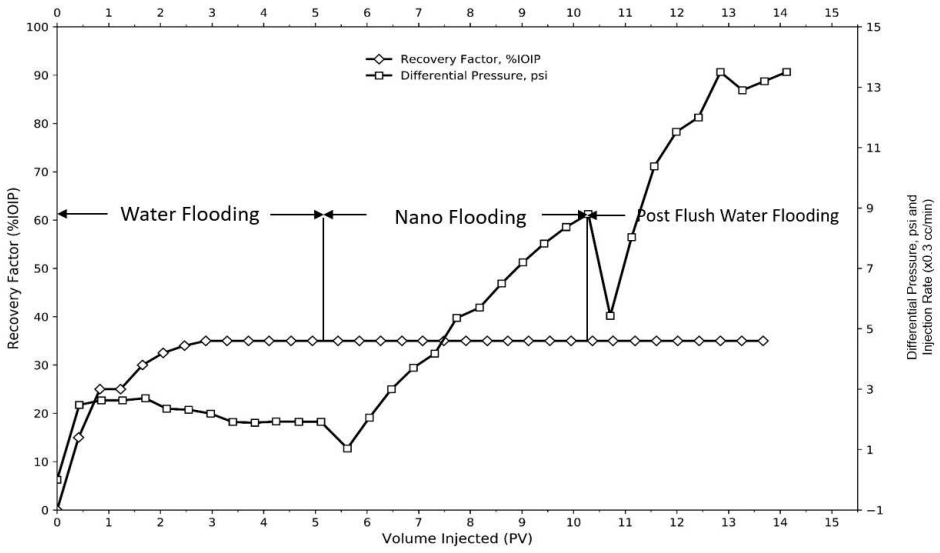

Figure 4.12. The core flooding test result of 0.5 wt% ST-AK NFs

Chapter 5

Numerical simulation of nano-solution EOR

This chapter provides information about numerical simulation with mathematical equations and formulas to predict the recovery mechanisms expected with the addition of nano-solution. This work carried out with the cooperation of Sugiyama (2019).

5.1 Introduction

Numerical simulation is an executed calculation utilizing a computer, following a program that applies mathematical models to a physical system. It is required to investigate the behavior of systems with complex mathematical models to provide numerical solutions mostly in non-linear systems. It has an advantage over analytic equations such that it does not require the assumptions that are inherent in traditional approaches. Also, in complex kinetic schemes, it can be safely used where the rate-determining step is not immediately apparent, such as a system involving multiple-tight binding interactions, and to mimic and match data over a broader range of experimental conditions and time scopes than is feasible with analytical equations. Numerical simulation of petroleum reservoir performance

refers to the construction and operation of a model whose behavior assumes the appearance of the actual reservoir and its behavior (Coats, 1987).

The model created itself is either physical (e.g., a laboratory sand-pack) or mathematical. A mathematical model is a set of equations that, subject to certain assumptions, describes the physical processes active in the reservoir. Although the model itself obviously lacks the reality of the reservoir, the behavior itself portrays a valid model of an actual reservoir. Numerical reservoir simulators are used extensively to simulate multi-phase and multi-component flow in a ”single porosity” reservoir. This research aims to develop a mathematical model to predict the oil recovery behavior by the addition of NPs referring to the experimental data.

5.2 Numerical simulation

A numerical simulator of nano-solution EOR was constructed referring to aluminosilicate NPs experimental data. According to the previous studies, due to the addition of NPs, the increase in oil recovery is caused not only by wettability alteration but also by structural disjoining pressure (Dehaghani and Daneshfar, 2019; Wijayanto et al., 2019). This pressure is considered to reduce residual oil as it separates the crude oil from the rock surfaces, and the driving mechanism is considered as the Brownian motion of the NPs and the electrical repulsion between the particles. The magnitude of the electrical repulsion that is believed to cause the disjoining pressure, which depends on the size of the NPs and the concentration of the NPs.

The numerical simulator was constructed comprehending the experimental results and assuming that the effects of the disjoining pressure were the primary mechanism, which occurs due to the addition of NPs. Therefore, to construct the nano-solution EOR simulator in this study, it requires the following functions:

(1) the estimation of disjoining pressure, changes in S_{or}, and relative permeability based on the intensity of disjoining pressure;

(2) calculating the agglomeration amount of NPs;

(3) changes in absolute permeability due to the agglomeration of NPs;

(4) the adsorption of NPs on the rock surface.

Constructing the numerical simulator requires governing equations, which are formulated based on oil in the oleic phase, and water and NPs in the aqueous phase. The governing equations can be expressed in Equations 5.1 to 5.3.

$$\frac{\partial}{\partial x}\left(\rho_{\mathrm{w,w}}\frac{kk_{\mathrm{rw}}}{\mu_{\mathrm{w}}}\frac{\partial P_{\mathrm{w}}}{\partial x}\right)+q_{\mathrm{w}}=\frac{\partial(N_{\mathrm{w}}\phi)}{\partial t} \tag{5.1}$$

$$\frac{\partial}{\partial x}\left(\rho_{\mathrm{NP,w}}\frac{kk_{\mathrm{rw}}}{\mu_{\mathrm{w}}}\frac{\partial P_{\mathrm{w}}}{\partial x}\right)+q_{\mathrm{NP}}=\frac{\partial(N_{\mathrm{NP}}\phi)}{\partial t} \tag{5.2}$$

$$\frac{\partial}{\partial x}\left(\rho_{\mathrm{o,o}}\frac{kk_{\mathrm{ro}}}{\mu_{\mathrm{w,o}}}\frac{\partial P_{\mathrm{o}}}{\partial x}\right)+q_{\mathrm{o}}=\frac{\partial(N_{\mathrm{o}}\phi)}{\partial t} \tag{5.3}$$

where $\rho_{\mathrm{w,w}}$ is molar density of water in water phase [mol/m^3], $\rho_{\mathrm{NP,w}}$ is molar density of NP in water phase [mol/m^3], $\rho_{\mathrm{o,o}}$ is molar density of oil in oil phase [mol/m^3], k is absolute permeability [m^2], k_{rw} is relative permeability of water [-], k_{ro} is relative permeability of oil [-], μ_{w} is viscosity of water [kg/(m.s)], $\mu_{\mathrm{w,o}}$ is viscosity of water in oil phase [kg/(m.s)], P_{w} is water phase pressure [kg/(m.s^2)], P_{o} is oil phase pressure [kg/(m.s^2)], q_{w} is mole rate of injected water per unit bulk volume [mol/(m^3.s)], q_{NP} is mole rate of injected NP per unit bulk volume [mol/(m^3.s)], q_{o} is mole rate of injected oil per unit bulk volume [mol/(m^3.s)], N_{w} is number of moles of water in unit bulk volume [mol/m^3], N_{NP} is number of moles of NP in unit bulk volume [mol/m^3], N_{o} number of moles of oil in unit bulk volume [mol/m^3], ϕ is porosity [-], x is one dimensional location [m], and t is time [s]..

With, $\rho_{\mathrm{w,w}}$ is number of moles of water per unit volume of water phase, $\rho_{\mathrm{NP,w}}$ is number of moles of NP per unit volume of water phase and $\rho_{\mathrm{o,o}}$ is number of moles of oil per unit volume of oil phase.

In addition to the above governing equations, several constitutive equations were incorporated into the simulator to express the phenomena associated with the injection of NPs, which are introduced below.

5.2.1 Disjoining pressure

The first step to construct the nano-EOR simulator's functions based on the intensity of disjoining pressure is the estimation of disjoining pressure, relative permeability, and S_{or} changes. The disjoining pressure depends on the size and concentration of NPs. Therefore, it is possible that there are "optimum" sizes and concentrations of these NPs,which maximize the disjoining pressure. The formula expresses disjoining pressure with the assumption that each NPs diameter and NPs concentration have an optimum value, which can be seen in Equation 5.4. The molar concentration of NPs shows that the disjoining pressure is a function of the effect of NP diameter (Figure 5.1) and concentration (Figure 5.2).

$$\Pi = a_{\text{dp}} \left(\frac{b_{\text{S}} S}{a_{\text{s}} S^4 + 1} \right) \left(\frac{b_{\text{C}} C}{a_{\text{C}} C^3 + 1} \right) \tag{5.4}$$

where Π is normalized disjoining pressure ($0 \leq \Pi \leq 1$)[-], C is concentration of NP [ppm], S is diameter of NP [nm], a_{dp} is an input parameter, a_{s} is an input parameter [1/nm^4], b_{S} is an input parameter [1/nm], a_{C} is an input parameter [1/ppm^3], and b_{C} is an input parameter [1/ppm].

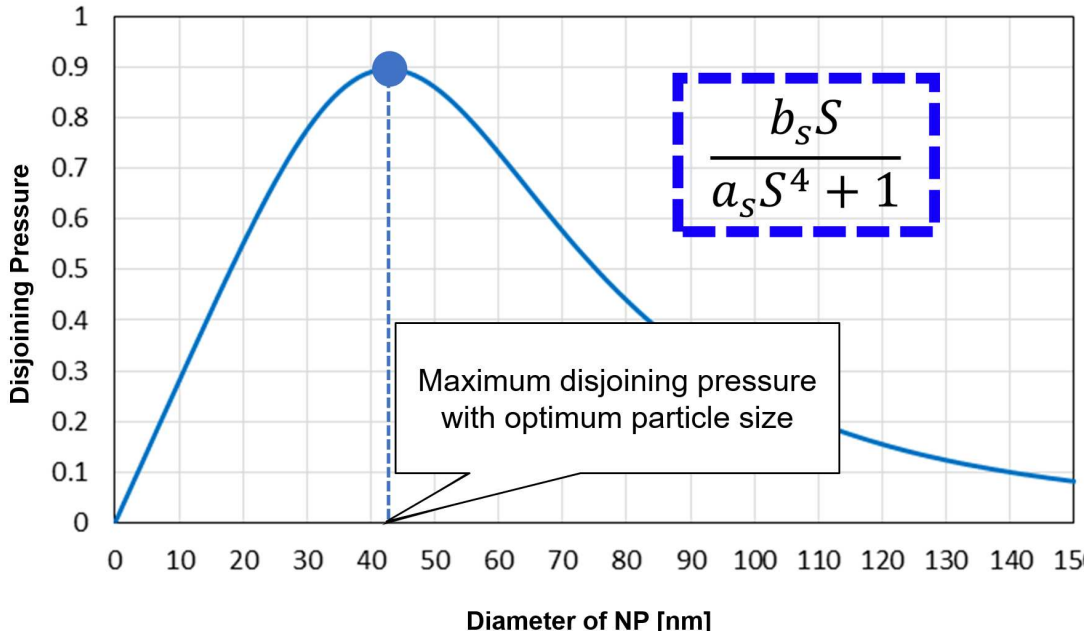

Figure 5.1. Relationship between NP diameter and disjoining pressure.

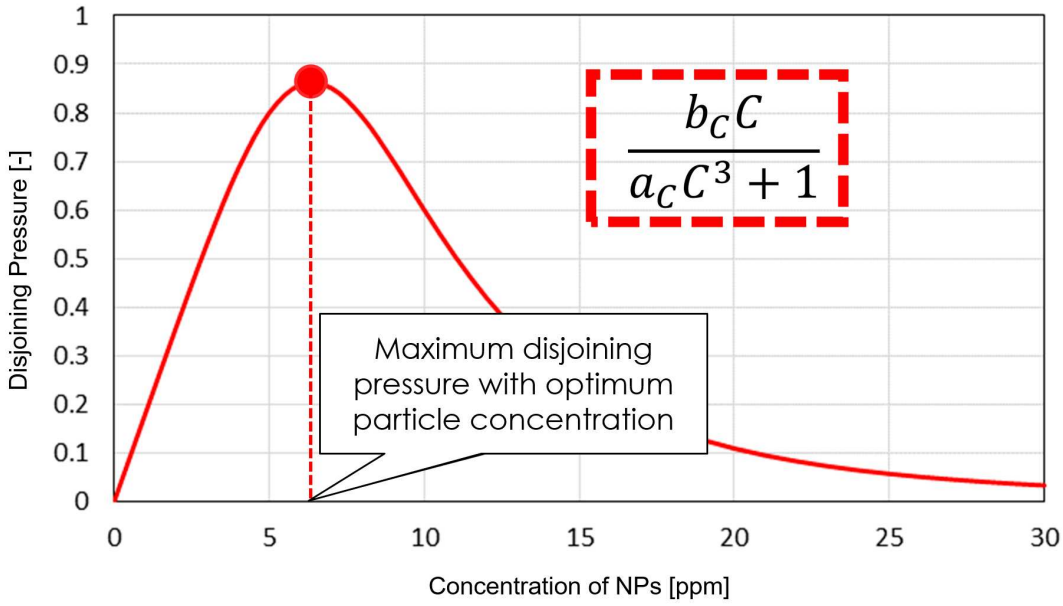

Figure 5.2. Relationship between NP concentration and disjoining pressure.

5.2.2 The adsorption of nanoparticles

The second step is to determine the amount of NPs adsorption on the rock surface using the Langmuir formula, which can be seen in Equation 5.5.

$$N_{\mathrm{NP_{ads}}} = min\left(N_{\mathrm{NP}}, \frac{aN_{\mathrm{NP}}}{1 + bN_{\mathrm{NP}}}\right) \tag{5.5}$$

where $N_{\mathrm{NP_{ads}}}$ is number of moles of NPs adsorbed on rock surface per unit bulk volume [mol/m^3], a is an input parameter [-], b is an input parameter [m^3/mol].

5.2.3 Relative permeability

At the third step, the relative permeability is determined using table data, depending on the disjoining pressure, and the amount of adsorption of NPs. There are two input data of relative permeability; one is with and the other is without the adsorption of NPs on a rock surface. Using these two data, the relative permeability is calculated as a function of $N_{\mathrm{NP_{ads}}}$ by linear interpolation, as represented in Equation 5.6.

$$k_{\mathrm{rl_{no\ DP}}} = k_{\mathrm{rl_{no\ ads}}}\left(1 - \frac{N_{\mathrm{NP_{ads}}}}{maxN_{\mathrm{NP_{ads}}}}\right) + k_{\mathrm{rl_{max\ ads}}}\left(\frac{N_{\mathrm{NP_{ads}}}}{maxN_{\mathrm{NP_{ads}}}}\right) \tag{5.6}$$

where $k_{\mathrm{rl_{no\ DP}}}$ is relative permeability to phase l at the stage where the disjoining pressure is not considered [-], $k_{\mathrm{rl_{no\ ads}}}$ is relative permeability to phase l at the stage where the adsorption of NPs is not considered [-], $k_{\mathrm{rl_{max\ ads}}}$ is relative permeability to phase l at the stage where the full adsorption of NPs is considered [-], $maxN_{\mathrm{NP_{ads}}}$ is maximum number of moles of NPs adsorbed on rock surface per unit bulk volume [mol/m^3].

The S_{or} can be also calculated without the effect of disjoining pressure, depending on the amount of adsorption of NPs as represented in Equation 5.7.

$$S_{\text{or}_{\text{no DP}}} = S_{\text{or}_{\text{no ads}}} \left(1 - \frac{N_{\text{NP}_{\text{ads}}}}{maxN_{\text{NP}_{\text{ads}}}}\right) + S_{\text{or}_{\text{max ads}}} \left(\frac{N_{\text{NP}_{\text{ads}}}}{maxN_{\text{NP}_{\text{ads}}}}\right) \tag{5.7}$$

where $S_{\text{or}_{\text{no DP}}}$ is S_{or} at the stage where the disjoining pressure is not considered [-], $S_{\text{or}_{\text{no ads}}}$ is S_{or} at the stage where the adsorption of NPs is not considered [-], $S_{\text{or}_{\text{max ads}}}$ is maximum S_{or} at the stage where the full adsorption of NPs is considered [-].

Then the k_{rw} and k_{ro} are calculated using Equation 5.8, with and without considering disjoining pressure, and the result can be observed in Figure 5.3. The disjoining pressure will occur if there are NPs.

$$S_{\text{or}} = (1 - \Pi) \times S_{\text{or}_{\text{noDP}}} + \Pi \times S_{\text{or}_{\text{maxDP}}} \tag{5.8}$$

where, $S_{\text{or}_{\text{maxDP}}}$ is S_{or} expected at the maximum of the disjoining pressure [-].

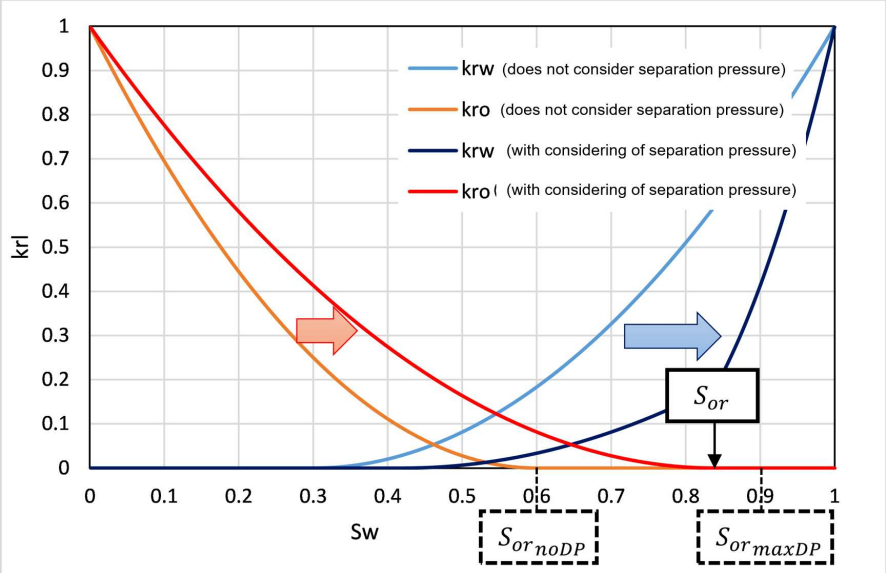

Figure 5.3. The conceptual diagram of change on relative permeability.

5.2.4 Agglomeration amount of nanoparticles

The fourth step is to estimate the agglomeration amount of NPs. There were two parameters considered to estimate the rate of NPs agglomeration in this research.

It was assumed that the agglomeration conditions would occur more likely with higher NP concentration and the smaller NP diameter, which is represented in Equation 5.9.

$$AP = \left(\frac{C}{C + a_1}\right)\left(\frac{b_1}{S - b_2} + b_3\right) \tag{5.9}$$

where AP is possibility of agglomeration [-], S is diameter of NP [nm], a_1 is an input data [ppm], b_1 is an input data [nm], b_2 is an input data [nm], and b_3 is an input data [-].

The formula for calculating the agglomeration rate is expressed in Equation 5.10.

$$V_{\mathrm{a_i}} = r \times \Delta t \times AP \times D_{\mathrm{NP_v}} \tag{5.10}$$

where $V_{\mathrm{a_i}}$ is NP agglomeration amount at timestep i [m^3], v_{r} is NP agglomeration kinetic constant [1/s], Δt is time increment in timestep i [s], and $D_{\mathrm{NP_v}}$ is Volume of NPs dispersed in the liquid [m^3].

The NPs will not disperse again once they agglomerate, and the amount of NPs agglomerated up to the ”n” time step can be calculated using following formula (Eq. 5.11). It can be inferred from the amount of NP agglomeration up to the n time step how much the porosity decreased.

$$V_{\mathrm{Agg_{total}}} = \sum_{i=1}^{n} V_{\mathrm{a_i}} \tag{5.11}$$

where $V_{\mathrm{Agg_{total}}}$ is the amount of NP agglomeration up to timestep n [m^3].

5.2.5 Absolute permeability

The last step to construct the nano-EOR simulator’s functions is to determine the changes in absolute permeability due to the NPs agglomeration. The porosity value is obtained using Equation 5.12 and then the absolute permeability is calculated using the Kozeny-Carman equation (Eq. 5.13).

$$\phi = \frac{V_{\text{pore}} - V_{\text{Agg}_{\text{total}}}}{V_{\text{control}}} \tag{5.12}$$

where ϕ is porosity [-], V_{pore} is volume pore without agglomeration of NP [m^3], V_{control} is control volume [m^3].

$$k = \alpha_{\text{perm}} \frac{\phi^3}{(1-\phi)^2} \tag{5.13}$$

where α_{perm} is an input parameter [m^2].

5.3 Simulation matching using experimental data

The core flooding experiments were carried out to observe the effects of NPs concentration on oil-increasing in flooding NPs, using NPs solutions of three different concentrations. The concentrations of NPs in the core flooding experiments 1, 2, and 3 are 1, 10, and 20 ppm, respectively, and were discussed in Chapter 3, section 3.2

The core plug used in the core flooding experiments were under different conditions in each of the experiments. The conditions and properties of the experiments are presented in Tables 5.1 and 5.2, respectively. Therefore, the relative permeability of each core was estimated from the cumulative oil production and differential pressure at the WF stage and can be observed in Figures 5.4 to 5.6.

Table 5.1. Conditions for each experiment.

Condition	**Value**
Particle size [nm]	90
Brine density [g/cm^3]	0.9985
Oil density [g/cm^3]	0.8702
Brine viscosity @ 60 °C [cP]	0.52
Oil viscosity @ 60 °C [cP]	19.97
Confining pressure [psig]	100
Experimental temperature [°C]	60
Injection rate [cm^3/min]	0.2

Table 5.2. The core properties used in core flooding experiments.

Properties	Exp.#1	Exp.#2	Exp.#3
Core length [cm]	3.54	3.54	3.52
Core diameter [cm]	2.545	2.545	2.545
Porosity [%]	19.74	19.76	19.33
Absolute permeability [mD]	374.7	386.7	359.1
Initial oil saturation rate [%]	82.08	82.84	84.58

*Exp.#: experiment number

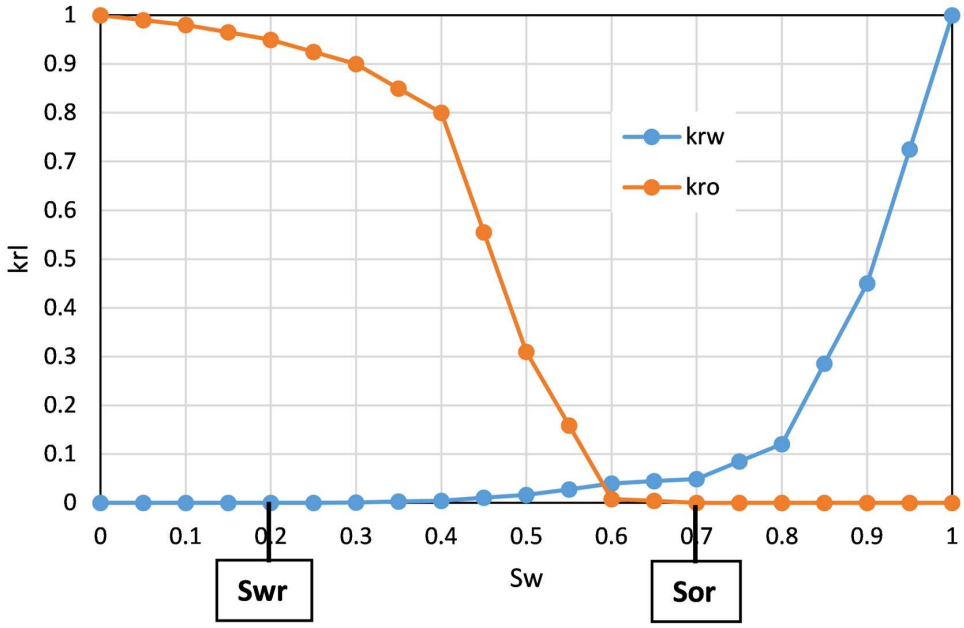

Figure 5.4. The relative permeability of 1 ppm aluminosilicate NPs.

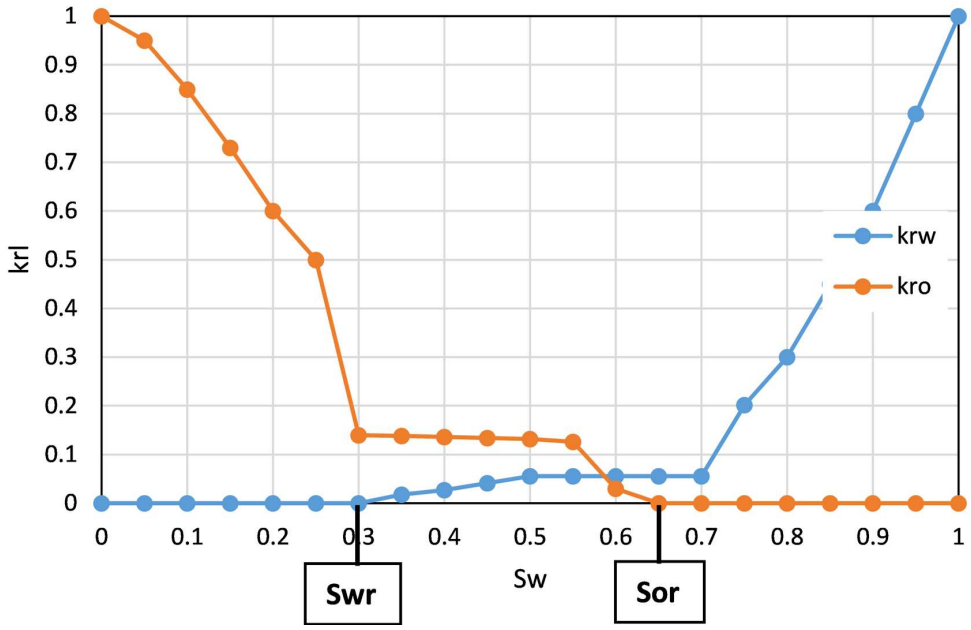

Figure 5.5. The relative permeability of 10 ppm aluminosilicateNPs.

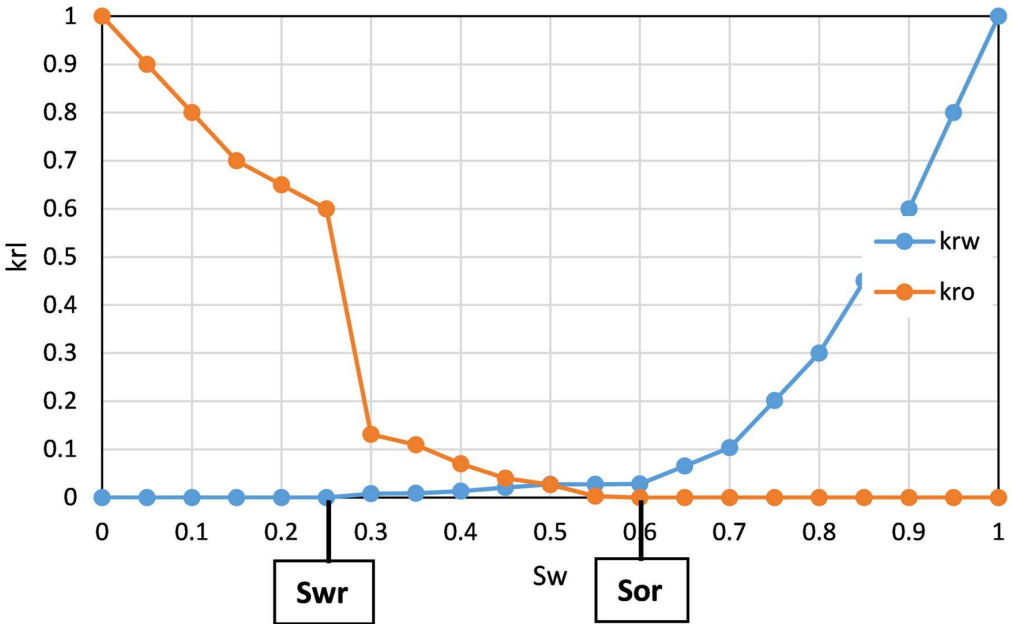

Figure 5.6. The relative permeability of 20 ppm aluminosilicate NPs.

Referring to the experimental data, a graph of the relationship between NPs concentration versus disjoining pressure was estimated, which is presented in Figure 5.7. It is shown that at the maximum disjoining pressure, the NPs concentration was estimated to be around 4.5-5 ppm. In order to verify the functions of the simulator developed in the above for predicting NPs-EOR behavior, these core flooding test were reproduced by simulations. The simulation model is shown in Figure 5.8. The input data including those regarding the disjoining pressure were optimized through simulation matching, as listed in Table 5.3.

Using the input data listed in Table 5.3 the core flooding experiments were simulated as depicted in Figures 5.9 to 5.14, which show the comparison of the cumulative oil production and the pressure difference for each experiment between the experimental and simulation results. In these figures, the blue line and red line show the simulation results for water injection and NPs injection periods, respectively, while the blue dot and the red dot indicate the experimental results for water injection and NPs injection periods, respectively.

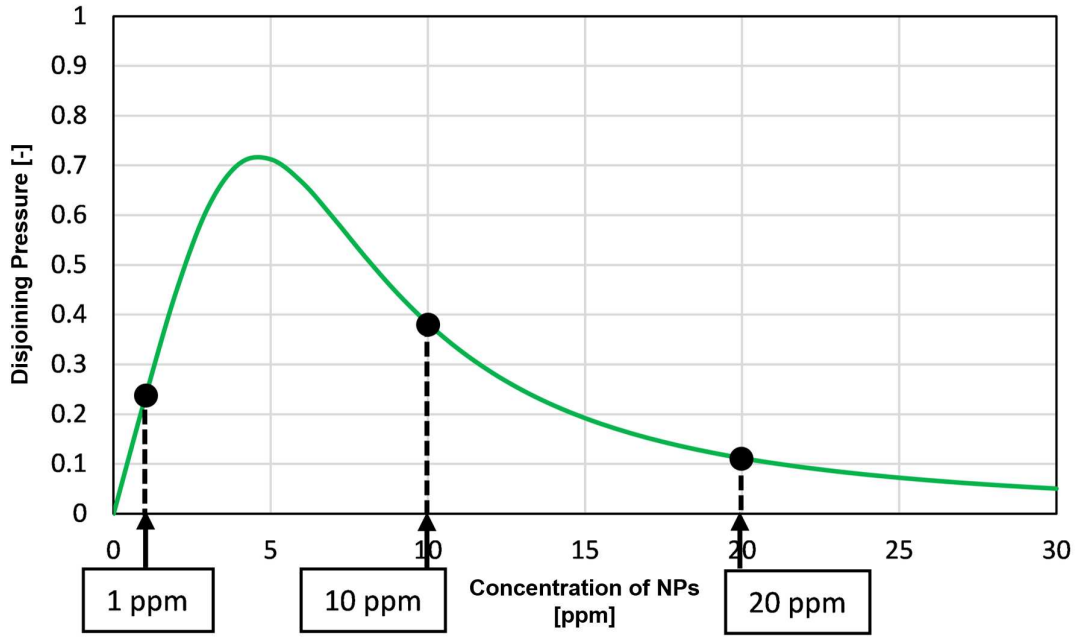

Figure 5.7. The relationship between NP concentration and disjoining pressure.

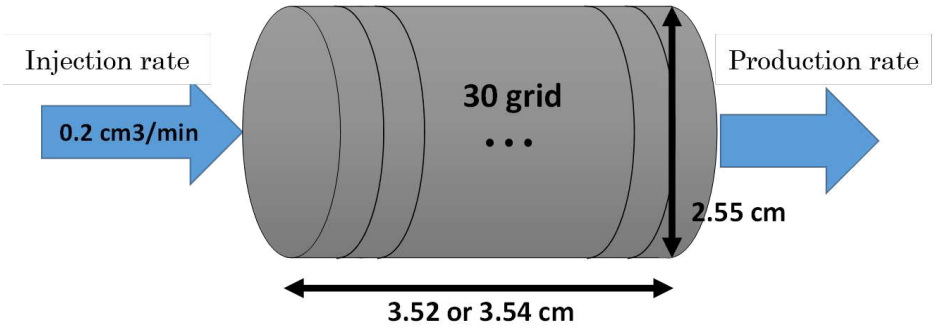

Figure 5.8. The simulation model.

Table 5.3. Input data of disjoining pressure.

Input data	Value
a_{DP}	2
a_S	0.0000001
b_S	0.031
a_C	0.0051
b_C	0.35
$S_{or_{noDP}}$	0.6
$S_{or_{maxDP}}$	0.9

Comparing the simulation results with the experimental data, it can be concluded that the cumulative oil production could be reproduced by simulation to some extent. In contrast, there some differences in the differential pressure be-

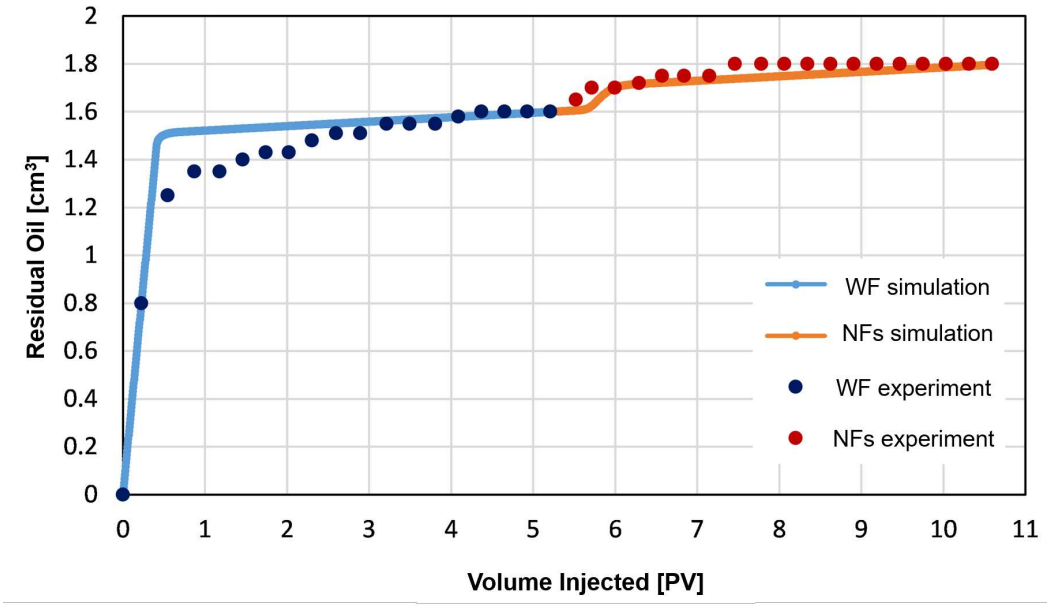

Figure 5.9. PV vs residual oil for 1 ppm aluminosilicate NPs

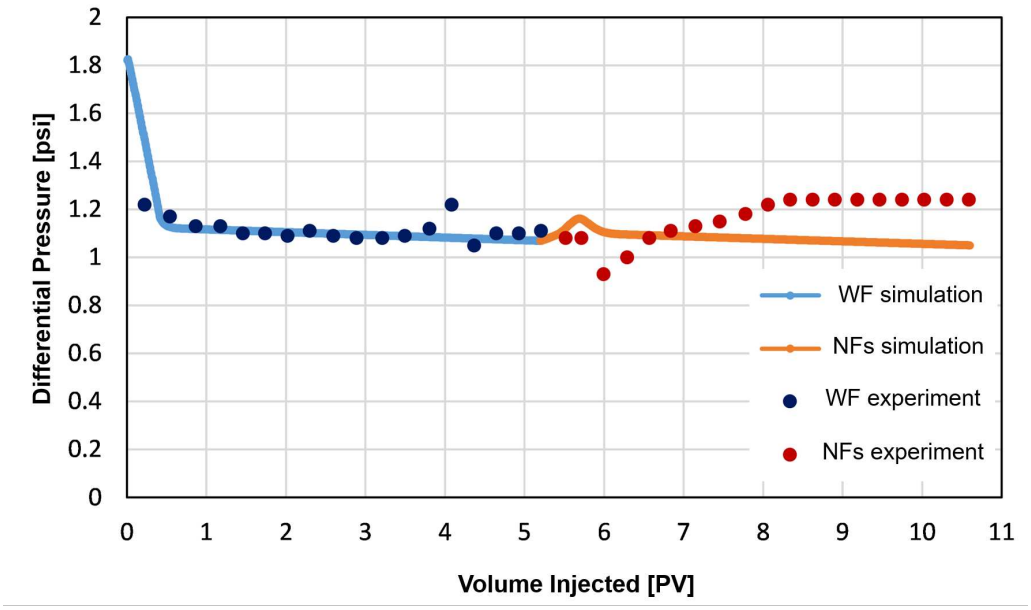

Figure 5.10. PV vs ΔP for 1 ppm aluminosilicate NPs

tween the simulation results and the experimental data, especially for the period after injecting the NPs in any experiment. In the experiments, the differential pressure increased or decreased depending on the experiment, while there was almost no change in the simulation. Therefore, it is not possible to make a simple discussion on the effects of injection of NPs on differential pressure. It is suggested that the differential pressure behavior may also be related to phenomena

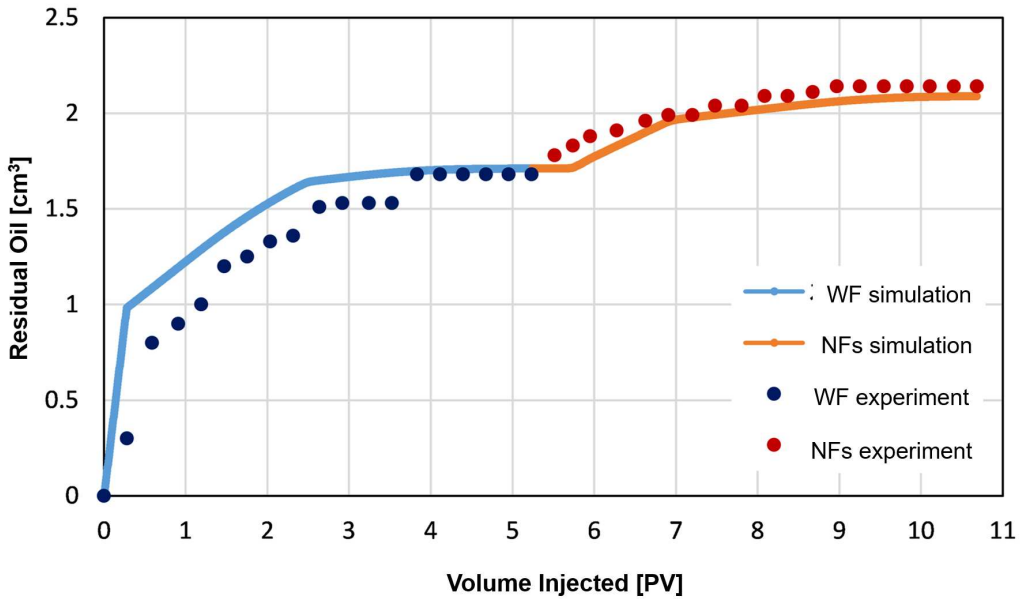

Figure 5.11. PV vs residual oil for 10 ppm aluminosilicate NPs

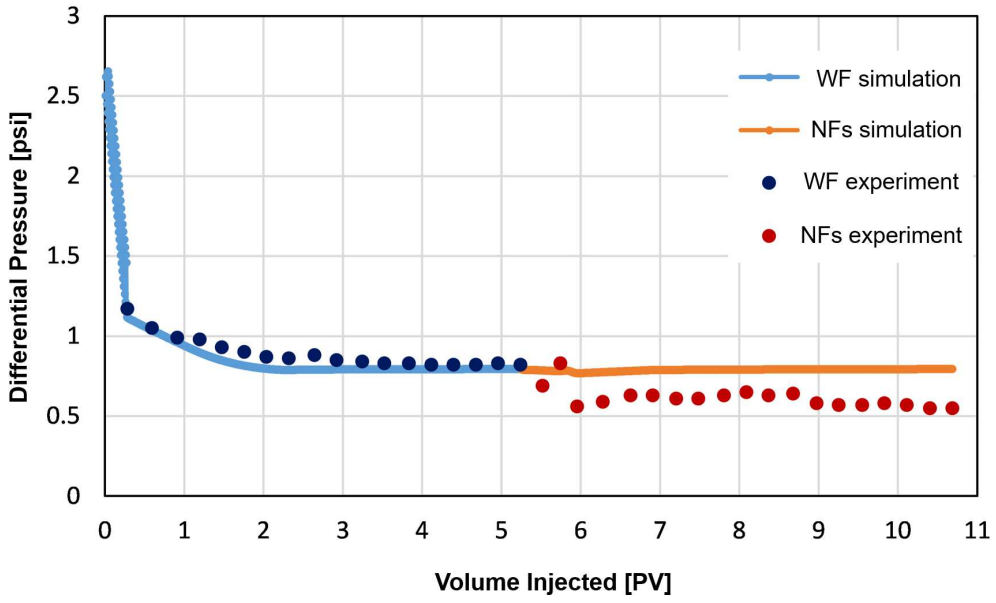

Figure 5.12. PV vs ΔP for 10 ppm aluminosilicate NPs.

such as adsorption and/or agglomeration of NPs depending on the concentration of NPs, and hence that further experiments and improvements in the simulator are required.

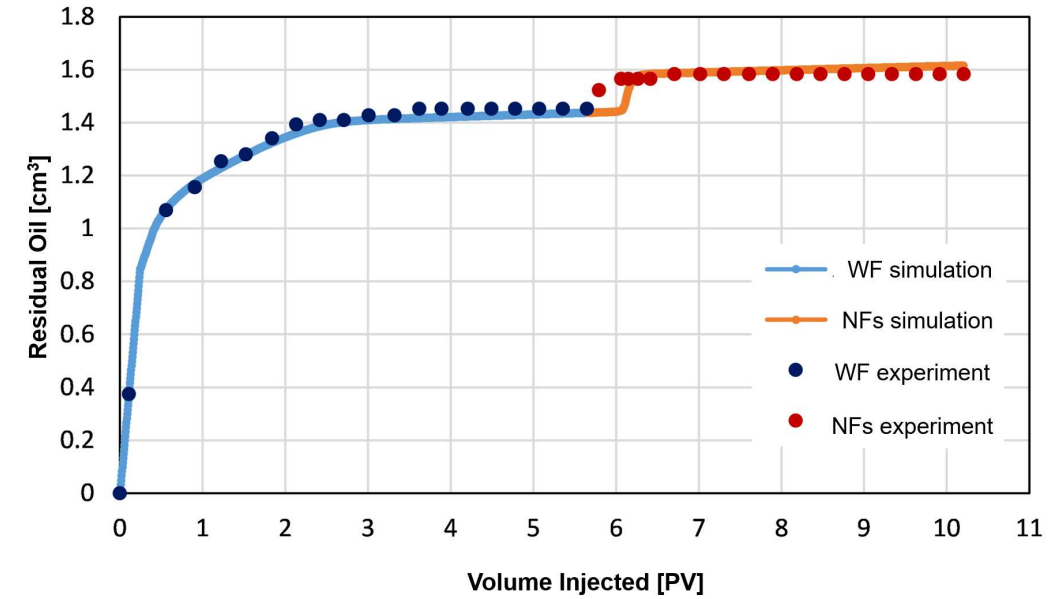

Figure 5.13. PV vs residual oil for 20 ppm aluminosilicate NPs.

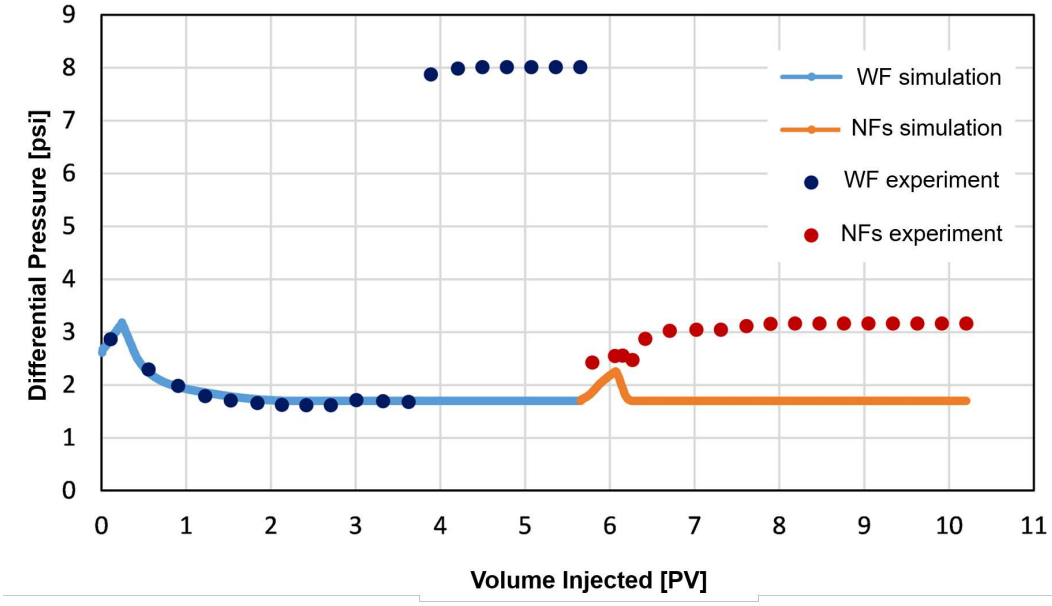

Figure 5.14. PV vs ΔP for 20 ppm aluminosilicate NPs.

Chapter 6

Conclusions and recommendation

This chapter summarizes the achievements of this research and provides recommendations for further additional research on the subject.

6.1 Conclusions

The ultimate objective of this research is to substantiate the applicability of NPs and to evaluate and recommend NPs as one of the emerging technologies in EOR methods, conducting experiments and simulation at a laboratory scale, prior to conducting field deployment. To attain this objective, the silica-alumina-based NPs were categorized and examined in the laboratory. This laboratory experimentation is an appropriate approach in explaining how NPs displace remaining or residual crude oil in porous media. The fluid properties analysis, IFT measurements, and wettability alteration observation were conducted to reveal the possible recovery mechanisms by NPs. In addition, core flooding experiments were conducted.

The aluminosilicate NPs solution was investigated from the viewpoints of its stability, WI, and IFT for cost-efficient EOR. The hydrophilic aluminosilicate of NPs can establish a stable water-wet reservoir environment and IFT reduction. The increase in the NFs concentration does not automatically result in recovering

higher incremental oil in low and medium permeability water-wet SS due to the fact that the core pore-throat can be blocked when the NPs are agglomerated. CMC assessment must be performed in order to properly evaluate the optimal concentration of NFs needed to achieve additional crude oil recovery.

The commercially available cationic-acidic ST-AK NFs were evaluated from the standpoints of IFT and wettability for a novel EOR application. The ST-AK NFs have the ability to change the wettability system from water-wet to stronger water-wet. However, they show a narrower effect of reducing the IFT between synthetic oil and NFs than that of the significance in IFT reduction performance by surfactant.

Core flooding experiments demonstrated that the aluminosilicate NPs and the ST-AK NFs were effective in dynamically recovering the residual crude oil. They generally perform to comply with very low concentration mixtures. On the contrary, at high concentrations, there is a possibility of agglomeration, which caused the blockage of the pore network. The highest incremental crude oil recoveries achieved were 15% with 10 ppm of aluminosilicate NPs solution and 9% with 0.0025 wt% of ST-AK NFs.

The numerical simulator was built, which incorporates the functions for reproducing the oil increase mechanisms using NPs. This simulator considers the agglomeration and the disjoining pressure of the NPs. Through the matching simulation with the experimental results, it was confirmed that the cumulative oil production could be reproduced to some extent.

The formation of NFs supports the advanced additional crude oil recovery. The influences of NFs injection on the increase in crude oil recovery were established from the above specific results. The driving or recovery mechanisms in NPs-EOR is envisaged to be the adsorption of the NFs that causes wettability alteration and the structural disjoining pressure.

6.2 Recommendations

This research expounds on the essential opinions in additional oil recovery processes by employing the media of NPs as a novel EOR agent of recovery. It also extends the understanding of oil recovery mechanisms by NFs and the various fluid-fluid and fluid-rock interactions. Nevertheless, additional investigations, including experimentation in applying bigger, longer, and different core samples such as carbonate core samples, pre and post-injection of NPs, are required to confirm the mechanisms identified in the current research.

The clarification of the oil recovery mechanisms by NFs was performed by analyzing the distribution of specific fluids at the pore level during nano flooding and should be further carried out in subsequent additional research phases. In the numerical simulation for matching with the experimental results, it was confirmed that the cumulative oil production could be reproduced to some extent. On the other hand, the differential pressure has not been sufficiently reproduced, and the simulator needs to be further improved.

Bibliography

Adil, M., Zaid, H. M., and Chuan, L. K. (2020). Electromagnetically-induced change in interfacial tension and contact angle of oil droplet using dielectric nanofluids. *Fuel*, 259:116274. 17

Afekare, D., Gupta, I., and Rao, D. (2020). Nanoscale investigation of silicon dioxide nanofluids and implications for enhanced oil recovery–an atomic force microscope study. *Journal of Petroleum Science and Engineering*, 191:107165. 16

Agista, M. N., Guo, K., and Yu, Z. (2018). A state-of-the-art review of nanoparticles application in petroleum with a focus on enhanced oil recovery. *Applied Sciences*, 8(6):871. 15

Al-Anssari, S., Wang, S., Barifcani, A., and Iglauer, S. (2017). Oil-water interfacial tensions of silica nanoparticle-surfactant formulations. *Tenside Surfactants Detergents*, 54(4):334–341. 30

Ali, J. A., Kolo, K., Manshad, A. K., and Stephen, K. D. (2019). Potential application of low-salinity polymeric-nanofluid in carbonate oil reservoirs: Ift reduction, wettability alteration, rheology and emulsification characteristics. *Journal of Molecular Liquids*, 284:735–747. xix, 50

Alnarabiji, M. S. and Husein, M. M. (2020). Application of bare nanoparticle-based nanofluids in enhanced oil recovery. *Fuel*, 267:117262. 55

Amott, E. (1959). Observations relating to the wettability of porous rock. *Petroleum Transactions, AIME*, 216:156–162. 22, 37

Amziane, S. and Collet, F. (2017). *Bio-aggregates based building materi-*

als: state-of-the-art report of the RILEM Technical Committee 236-BBM, volume 23. Springer. 20, 21, 22

Anderson, W. G. (1987). Wettability literature survey-part 6: the effects of wettability on waterflooding. *Journal of Petroleum Technology*, 39(12):1–605. 22, 40, 49

Andreassen, L. (2015). *Nanoparticle effect on interfacial properties related to Enhanced Oil Recovery*. Master's thesis, NTNU. 9

API (1968). *Recommended practice for analysis of oil-field waters*, volume 45. American Petroleum Institute, Production Dept. 26

ASTM, D.-. (1995). *Standard Test Method for Acid Number of Petroleum Products by Potentiometric Titration*. D664-95 ASTM International West Conshohocken, PA. 25

ASTM, D.-. (2011). *Standard Test Method for Base Number of Petroleum Products by Potentiometric Perchloric Acid Titration*. D2896-15 ASTM West Conshohocken, PA, USA. 25

Aurand, K. (2015). Using nanofluids to enhance oil recovery. *NTNU TechZone*, 3. 14

Baroña, G. N. B., Lim, J., Choi, M., and Jung, B. (2013). Interfacial polymerization of polyamide-aluminosilicate swnt nanocomposite membranes for reverse osmosis. *Desalination*, 325:138–147. 8

Barron, A. (2010). The early history of nanotechnology. *Connexions*. 2

Belkin, A., Hubler, A., and Bezryadin, A. (2015). Self-assembled wiggling nanostructures and the principle of maximum entropy production. *Scientific Reports*, 5:8323. 2

Betancur, S., Giraldo, L. J., Carrasco-Marin, F., Riazi, M., Manrique, E. J., Quintero, H., Garia, H. A., Franco-Ariza, C. A., and Cortes, F. B. (2019). Importance of the nanofluid preparation for ultra-low interfacial tension in enhanced oil recovery based on surfactant–nanoparticle–brine system interaction. *ACS omega*, 4(14):16171–16180. 53

Buckley, J. S. and Fan, T. (2007). Crude oil/brine interfacial tensions1. *Petrophysics*, 48(03). 15

Buongiorno, J. (2006). Convective transport in nanofluids. *Journal of heat transfer*, 128(3):240–250. 3

Chaudhury, M. (2003). Complex fluids: Spread the word about nanofluids. *Nature*, 423(6936):131. 49

Chen, James (2019). Crude oil-black gold defined. https://www.investopedia.com/terms/c/crude-oil.asp, Last accessed on 2019-12-6. 24

Chengara, A., Nikolov, A. D., Wasan, D. T., Trokhymchuk, A., and Henderson, D. (2004). Spreading of nanofluids driven by the structural disjoining pressure gradient. *Journal of Colloid and Interface Science*, 280(1):192–201. 16

Cheraghian, G., Hemmati, M., Masihi, M., and Bazgir, S. (2013). An experimental investigation of the enhanced oil recovery and improved performance of drilling fluids using titanium dioxide and fumed silica nanoparticles. *Journal of Nanostructure in Chemistry*, 3(1):78. 14

Cheraghian, G., Kiani, S., Nassar, N. N., Alexander, S., and Barron, A. R. (2017). Silica nanoparticle enhancement in the efficiency of surfactant flooding of heavy oil in a glass micromodel. *Industrial & Engineering Chemistry Research*, 56(30):8528–8534. 3, 14

Chung, J., Boudouris, B. W., and Franses, E. I. (2018). Surface tension behavior of aqueous solutions of a propoxylated surfactant and interfacial tension behavior against a crude oil. *Colloids and Surfaces A: Physicochemical and Engineering Aspects*, 537:163–172. 48

Clarke, A., Howe, A. M., Mitchell, J., Staniland, J., and Hawkes, L. A. (2016). How viscoelastic-polymer flooding enhances displacement efficiency. *SPE Journal*, 21(03):675–687. 27

Coats, K. (1987). Reservoir simulation//petroleum engineering handbook. 62

Das, S., Choi, S., Yu, W., and Pradeep, T. (2007). *Nanofluids: science and technology*. John Wiley & Sons. 3, 4, 7, 10, 14, 36

Degabriel, T., Colaço, E., Domingos, R. F., El Kirat, K., Brouri, D., Casale, S., Landoulsi, J., and Spadavecchia, J. (2018). Factors impacting the aggregation/agglomeration and photocatalytic activity of highly crystalline spheroid- and rod-shaped tio 2 nanoparticles in aqueous solutions. *Physical Chemistry Chemical Physics*, 20(18):12898–12907. 29

Dehaghani, A. H. S. and Daneshfar, R. (2019). How much would silica nanoparticles enhance the performance of low-salinity water flooding? *Petroleum Science*, 16(3):591–605. 55, 62

DESA, U. (2019). World population prospects 2019: Highlights. *New York (US): United Nations Department for Economic and Social Affairs*. 1

Donaldson, E., Thomas, R., and Lorenz, P. (1969). Wettability determination and its effect on recovery efficiency. *Society of Petroleum Engineers Journal*, 9(01):13–20. 22

Drelich, J., Fang, C., and White, C. (2002). Measurement of interfacial tension in fluid-fluid systems. *Encyclopedia of Surface and Colloid Science*, 3:3158–3163. 21

Drexler, K. E. (2001). Machine-phase nanotechnology. *Scientific American*, 285(3):66–7. 7

Druetta, P. and Picchioni, F. (2019). Polymer and nanoparticles flooding as a new method for enhanced oil recovery. *Journal of Petroleum Science and Engineering*, 177:479–495. 11

Dunphy Guzmán, K. A., Taylor, M. R., and Banfield, J. F. (2006). Environmental risks of nanotechnology: National nanotechnology initiative funding, 2000-2004. 2

Ehtesabi, H., Ahadian, M. M., Taghikhani, V., and Ghazanfari, M. H. (2013). Enhanced heavy oil recovery in sandstone cores using tio2 nanofluids. *Energy & Fuels*, 28(1):423–430. 14

Faghri, A. and Zhang, Y. (2006). *Transport phenomena in multiphase systems*. Elsevier. 15

Feynman, R. P. (1959). Plenty of room at the bottom. In *APS annual meeting*. 7, 8

Fletcher, A. and Davis, J. (2010). How eor can be transformed by nanotechnology. In *SPE Improved Oil Recovery Symposium*. Society of Petroleum Engineers. 12

Fuseni, A., Han, M., and Al-Mobith, A. (2013). Phase behavior and interfacial tension properties of an amphoteric surfactant for eor application. In *SPE Saudi Arabia section technical symposium and exhibition*. Society of Petroleum Engineers. 49

Gao, B. and Sharma, M. M. (2013). A family of alkyl sulfate gemini surfactants. 2. water–oil interfacial tension reduction. *Journal of Colloid and Interface Science*, 407:375–381. 49

Giraldo, J., Benjumea, P., Lopera, S., Cortés, F. B., and Ruiz, M. A. (2013). Wettability alteration of sandstone cores by alumina-based nanofluids. *Energy & Fuels*, 27(7):3659–3665. 3, 16, 24, 37, 38

Green, D. W. and Willhite, G. P. (1998). *Enhanced oil recovery*, volume 6. Henry L. Doherty Memorial Fund of AIME, Society of Petroleum Engineers. 19, 21, 48, 49

Guerriero, V., Mazzoli, S., Iannace, A., Vitale, S., Carravetta, A., and Strauss, C. (2013). A permeability model for naturally fractured carbonate reservoirs. *Marine and Petroleum Geology*, 40:115–134. 18

Hamaker, H. C. (1937). The london—van der waals attraction between spherical particles. *physica*, 4(10):1058–1072. 36

Healy, T. W. (2006). Stability of aqueous silica sols. *Surfactant science series*, 131:247–252. 29

Hendraningrat, L. (2015). *Unlocking the Potential of Hydrophilic Nanoparticles as Novel Enhanced Oil Recovery Method: An Experimental Investigation*. PhD thesis, Norwegian University of Science and Technology (NTNU). 12, 48, 55

Hendraningrat, L., Li, S., and Torsæter, O. (2013a). A coreflood investigation of nanofluid enhanced oil recovery. *Journal of Petroleum Science and Engineer-*

ing, 111:128–138. 3, 14, 41, 54

Hendraningrat, L., Li, S., and Torsaeter, O. (2013b). A coreflood investigation of nanofluid enhanced oil recovery in low-medium permeability berea sandstone. In *SPE International Symposium on Oilfield Chemistry*. OnePetro. 17

Hendraningrat, L., Li, S., and Torsæter, O. (2013c). Effect of some parameters influencing enhanced oil recovery process using silica nanoparticles: an experimental investigation. In *SPE Reservoir Characterization and Simulation Conference and Exhibition*. OnePetro. 39, 48

Hendraningrat, L., Li, S., and Torsæter, O. (2013d). Enhancing oil recovery of low-permeability berea sandstone through optimised nanofluids concentration. In *SPE Enhanced Oil Recovery Conference*. Society of Petroleum Engineers. 41

Hendraningrat, L. and Torsæter, O. (2014). Effects of the initial rock wettability on silica-based nanofluid-enhanced oil recovery processes at reservoir temperatures. *Energy & Fuels*, 28(10):6228–6241. 38

Hite, J. and Bondor, P. (2004). Planning eor projects. In *SPE International Petroleum Conference in Mexico*. Society of Petroleum Engineers. 1

Houston, S. (2007). *Formation waters in petroleum reservoirs; their controls and applications*. PhD thesis, The University of Leeds, School of Earth and Environment, pp. 240. 25, 45

Howard, P. H., Sage, G., Jarvis, W., and Gray, D. (1990). *Handbook of environmental fate and exposure data for organic chemicals. Volume II: solvents*. Chelsea, MI (US); Lewis Publishers, Inc. 40, 47

Hu, Z., Azmi, S. M., Raza, G., Glover, P. W., and Wen, D. (2016). Nanoparticle-assisted water-flooding in berea sandstones. *Energy & Fuels*, 30(4):2791–2804. 36

Idogun, A., Iyagba, E., Ukwotije-Ikwut, R., and Aseminaso, A. (2016). A review study of oil displacement mechanisms and challenges of nanoparticle enhanced oil recovery. In *SPE Nigeria Annual International Conference and Exhibition*.

Society of Petroleum Engineers. 49

Iijima, S. (1991). Helical microtubules of graphitic carbon. *Nature*, 354(6348):56–58. 7

ISO, T. (2007). 80004-1: Nanotechnologies-vocabulary-part 1: Core terms. 2007. *International Standards Organization, Geneva, Switzerland*. 8

Jafari, S., He, Y., and Bhandari, B. (2006). Nano-emulsion production by sonication and microfluidization—a comparison. *International Journal of Food Properties*, 9(3):475–485. 27

Jarvie, H., King, S., and Dobson, P. (2019). Nanoparticle. https://www.britannica.com/science/nanoparticle. 9

Jenkins, R. (1999). *X-ray fluorescence spectrometry*, volume 2. Wiley New York. 26

Jenkins, S., Kirk, S. R., Persson, M., Carlen, J., and Abbas, Z. (2007). Molecular dynamics simulation of nanocolloidal amorphous silica particles: part i. *The Journal of chemical physics*, 127(22):224711. 29

Jenkins, S., Kirk, S. R., Persson, M., Carlen, J., and Abbas, Z. (2008). Molecular dynamics simulation of nanocolloidal amorphous silica particles: Part ii. *The Journal of chemical physics*, 128(16):164711. 29

Jia, H., Song, Y., Jiang, D., Xing, L., Leng, X., Zhu, Y., An, J., Dong, A., Jia, C., and Zhou, H. (2017). Systematic investigation of the synergistic effects of novel biosurfactant ethoxylated phytosterol-alcohol systems on the interfacial tension of a water/model oil system. *Colloids and Surfaces A: Physicochemical and Engineering Aspects*, 513:292–296. 49

Jiang, R., Li, K., and Horne, R. (2017). A mechanism study of wettability and interfacial tension for eor using silica nanoparticles. In *SPE Annual Technical Conference and Exhibition*. Society of Petroleum Engineers. 49

Joonaki, E. and Ghanaatian, S. (2014). The application of nanofluids for enhanced oil recovery: effects on interfacial tension and coreflooding process. *Petroleum Science and Technology*, 32(21):2599–2607. 41

Kazemzadeh, Y., Shojaei, S., Riazi, M., and Sharifi, M. (2019). Review on application of nanoparticles for eor purposes: A critical review of the opportunities and challenges. *Chinese Journal of Chemical Engineering*, 27(2):237–246. 15

Keller, A. A., Wang, H., Zhou, D., Lenihan, H. S., Cherr, G., Cardinale, B. J., Miller, R., and Ji, Z. (2010). Stability and aggregation of metal oxide nanoparticles in natural aqueous matrices. *Environmental science & technology*, 44(6):1962–1967. 10, 16

Khan, M. R. and Rizvi, T. F. (2014). Nanotechnology: scope and application in plant disease management. *Plant Pathol J*, 13(3):214–231. 14

Kissa, E. (2017). *Dispersions: characterization, testing, and measurement*. Routledge. 29

Ko, S., Lee, H., and Huh, C. (2017). Efficient removal of enhanced-oil-recovery polymer from produced water with magnetic nanoparticles and regeneration/reuse of spent particles. *SPE Production & Operations*, 32(03):374–381. 54

Kong, X. and Ohadi, M. (2010). Applications of micro and nano technologies in the oil and gas industry-overview of the recent progress. In *Abu Dhabi international petroleum exhibition and conference*. Society of Petroleum Engineers. 2, 8, 10

Kuang, W., Saraji, S., and Piri, M. (2018). A systematic experimental investigation on the synergistic effects of aqueous nanofluids on interfacial properties and their implications for enhanced oil recovery. *Fuel*, 220:849–870. 36, 52

Lake, L. W. (1989). *Enhanced oil recovery*. Old Tappan, NJ; Prentice Hall Inc. 12

Li, S., Kaasa, A., Hendraningrat, L., and Torsæter, O. (2013). Effect of silica nanoparticles adsorption on the wettability index of berea sandstone. In *Paper SCA2013-059 presented at the international symposium of the society of core analysts held in Napa Valley, California, USA*, pages 16–19. 39

Li, S. and Torsæter, O. (2014). An experimental investigation of eor mechanisms

for nanoparticles fluid in glass micromodel. In *Paper SCA2014-022 was prepared for presentation at the International Symposium of the Society of Core Analysts held in Avignon, France*, pages 8–11. 3, 38, 49

Liu, P., Li, X., Yu, H., Niu, L., Yu, L., Ni, D., and Zhang, Z. (2020). Functional janus-sio$_2$ nanoparticles prepared by a novel "cut the gordian knot" method and their potential application for enhanced oil recovery. *ACS Applied Materials & Interfaces*, 12(21):24201–24208. 55

Mahbubul, I., Chong, T. H., Khaleduzzaman, S., Shahrul, I., Saidur, R., Long, B., and Amalina, M. (2014). Effect of ultrasonication duration on colloidal structure and viscosity of alumina–water nanofluid. *Industrial & Engineering Chemistry Research*, 53(16):6677–6684. 3

Mandal, A. and Bera, A. (2012). Surfactant stabilized nanoemulsion: characterization and application in enhanced oil recovery. *International Journal of Chemical and Molecular Engineering*, 6(7):537–542. 39

Mandal, A., Samanta, A., Bera, A., and Ojha, K. (2010). Characterization of oil-water emulsion and its use in enhanced oil recovery. *Industrial & Engineering Chemistry Research*, 49(24):12756–12761. 34, 51

Marsden, S., Ramey, H., and Sanyal, S. (1973). The effect of temperature on electrical resistivity of porous media. *The Log Analyst*, 14(02). 22

MEMR, P. (2018). Handbook of energy and economic statistics of indonesia 2018. *Kementerian Energi Dan Sumber Daya Mineral Republik Indonesia (MEMR). Jakarta*. 1

Metin, C. O., Baran, J. R., and Nguyen, Q. P. (2012). Adsorption of surface functionalized silica nanoparticles onto mineral surfaces and decane/water interface. *Journal of Nanoparticle Research*, 14(11):1246. 3, 14, 24, 53

Minkowycz, W., Sparrow, E., and Abraham, J. P. (2016). *Nanoparticle heat transfer and fluid flow*. CRC press. 10

Miranda, C., Lara, L., and Tonetto, B. (2012). Stability and mobility of functionalized silica nanoparticles for enhanced oil recovery applications. In *SPE*

International Oilfield Nanotechnology Conference and Exhibition. Society of Petroleum Engineers. 2, 3, 14, 24

Mokhatab, S., Fresky, M. A., and Islam, M. R. (2006). Applications of nanotechnology in oil and gas e&p. *Journal of Petroleum Technology*, 58(04):48–51. 8

Morgan, W. B. and Pirson, S. J. (1964). The effect of fractional wettability on the archie saturation exponent. In *SPWLA 5th Annual Logging Symposium*. Society of Petrophysicists and Well-Log Analysts. 22

Morrow, N. R. (1990). Wettability and its effect on oil recovery. *Journal of Petroleum Technology*, 42(12):1–476. 15, 20, 22, 49, 56

Nanowerk (2020). Nanoparticle production – how nanoparticles are made. https://www.nanowerk.com/how_nanoparticles_are_made.php. 26

Ogolo, N., Olafuyi, O., and Onyekonwu, M. (2012). Enhanced oil recovery using nanoparticles. In *SPE Saudi Arabia section technical symposium and exhibition*. Society of Petroleum Engineers. 3, 14, 24

Parvazdavani, M., Masihi, M., and Ghazanfari, M. (2014). Monitoring the influence of dispersed nano-particles on oil–water relative permeability hysteresis. *Journal of Petroleum Science and Engineering*, 124:222–231. 39

Peng, B., Zhang, L., Luo, J., Wang, P., Ding, B., Zeng, M., and Cheng, Z. (2017). A review of nanomaterials for nanofluid enhanced oil recovery. *RSC Advances*, 7(51):32246–32254. 39

Potts, D. and Kuehne, D. (1988). Strategy for alkaline/polymer flood design with berea and reservoir-rock corefloods. *SPE Reservoir Engineering*, 3(04):1–143. 48

Rao, Y. (2010). Nanofluids: stability, phase diagram, rheology and applications. *Particuology*, 8(6):549–555. 3, 10, 11, 36, 46

Robson, S., Abdassah, D., Thaib, N., Hidayat, D., and Rist, S. (2005). A strategy for the revitalisation of indonesian brownfields. In *IPA Conference and Exhibition*. Indonesian Petroleum Association. 1

Sagala, F., Hethnawi, A., and Nassar, N. N. (2020). Hydroxyl-functionalized silicate-based nanofluids for enhanced oil recovery. *Fuel*, 269:117462. 52, 53

Saleh, N., Kim, H.-J., Phenrat, T., Matyjaszewski, K., Tilton, R. D., and Lowry, G. V. (2008). Ionic strength and composition affect the mobility of surface-modified fe0 nanoparticles in water-saturated sand columns. *Environmental Science & Technology*, 42(9):3349–3355. 36

Skauge, T., Spildo, K., and Skauge, A. (2010). Nano-sized particles for eor. In *SPE improved oil recovery symposium*. Society of Petroleum Engineers. 18

Smith, J. T. and Cobb, W. M. (1997). *Waterflooding*. Midwest Office of the Petroleum Technology Transfer Council. 52

Sofla, S. J. D., James, L. A., and Zhang, Y. (2018). Insight into the stability of hydrophilic silica nanoparticles in seawater for enhanced oil recovery implications. *Fuel*, 216:559–571. 16

Sondenaa, E., Bratteli, F., Normann, H., and Kollveit, K. (1991). The effect of reservoir conditions, and wettability on electrical resistivity. In *SPE Asia-Pacific Conference*. Society of Petroleum Engineers. 22

Sugiyama, S. (2019). *Development of simulator for predicting performance of micro emulsion and EOR using nanoparticle*. Master's thesis, Department of Earth Sciences, Resources, and Environmental Engineering, Graduate School of Creative Science and Engineering, Waseda University. 61

Taniguchi, N. (1974). On the basic concept of 'nano-technology'. In *Proceedings of the International Conference of Production Engineering Japan Society of Precision Engineering*. Tokyo. 7

Vert, M., Doi, Y., Hellwich, K., Hess, M., Hodge, P., Kubisa, P., Rinaudo, M., and Schué, F. (2012). Terminology for biorelated polymers and applications (iupac recommendations 2012). *Pure and Applied Chemistry*, 84(2):377–410. 8

Vignati, E., Piazza, R., and Lockhart, T. P. (2003). Pickering emulsions: interfacial tension, colloidal layer morphology, and trapped-particle motion. *Langmuir*, 19(17):6650–6656. 53

Vonnegut, B. (1942). Rotating bubble method for the determination of surface and interfacial tensions. *Review of Scientific Instruments*, 13(1):6–9. 33

Wan, R. (2011). *Advanced well completion engineering*. Gulf professional publishing. 25

Wasan, D., Nikolov, A., and Kondiparty, K. (2011). The wetting and spreading of nanofluids on solids: Role of the structural disjoining pressure. *Current Opinion in Colloid and Interface Science*, 16(4):344–349. xix, 16

White, W. B. (2012). Hydrogeology of karst aquifers. In *Encyclopedia of caves*, pages 383–391. Elsevier. 18

Wijayanto, T., Kurihara, M., Kurniawan, T., and Muraza, O. (2019). Experimental investigation of aluminosilicate nanoparticles for enhanced recovery of waxy crude oil. *Energy & Fuels*, 33(7):6076–6082. 52, 53, 55, 62

Wikipedia (2020). Brine — Wikipedia, the free encyclopedia. https://en.wikipedia.org/w/index.php?title=Brine&oldid=996600123. [Online; accessed 30-December-2020]. 45, 46

Wu, W., He, Q., and Jiang, C. (2008). Magnetic iron oxide nanoparticles: synthesis and surface functionalization strategies. *Nanoscale Research Letters*, 3(11):397. 16

Xie, H., Yu, W., and Chen, W. (2010). Mgo nanofluids: higher thermal conductivity and lower viscosity among ethylene glycol-based nanofluids containing oxide nanoparticles. *Journal of Experimental Nanoscience*, 5(5):463–472. 4

Xie, Y., Khishvand, M., and Piri, M. (2020). Impact of connate brine chemistry on in situ wettability and oil recovery: Pore-scale experimental investigation. *Energy & Fuels*, 34(4):4031–4045. 55

Yekeen, N., Padmanabhan, E., Syed, A. H., Sevoo, T., and Kanesen, K. (2020). Synergistic influence of nanoparticles and surfactants on interfacial tension reduction, wettability alteration and stabilization of oil-in-water emulsion. *Journal of Petroleum Science and Engineering*, 186:106779. 54

Yousefvand, H. A. and Jafari, A. (2018). Stability and flooding analysis of

nanosilica/nacl/hpam/sds solution for enhanced heavy oil recovery. *Journal of Petroleum Science and Engineering*, 162:283–291. 36

Yu, W. and Xie, H. (2012). A review on nanofluids: preparation, stability mechanisms, and applications. *Journal of Nanomaterials*, 2012:1. 9, 11, 27, 36

Zargartalebi, M., Barati, N., and Kharrat, R. (2014). Influences of hydrophilic and hydrophobic silica nanoparticles on anionic surfactant properties: Interfacial and adsorption behaviors. *Journal of Petroleum Science and Engineering*, 119:36–43. 3, 14

Zhang, H., Nikolov, A., and Wasan, D. (2014). Enhanced oil recovery (eor) using nanoparticle dispersions: underlying mechanism and imbibition experiments. *Energy & Fuels*, 28(5):3002–3009. 9

Zhang, H., Ramakrishnan, T., Nikolov, A., and Wasan, D. (2018). Enhanced oil displacement by nanofluid's structural disjoining pressure in model fractured porous media. *Journal of Colloid and Interface Science*, 511:48–56. 17

A. Imbibition process of aluminosilicate NPs

Figures 1 to 7 shows the imbibition process from day 0 to day 6, respectively. Figures 8 and 9 shows the core condition during the imbibition process.

Figure 1. The imbibition process, Day 0.

Figure 2. The imbibition process, Day 1.

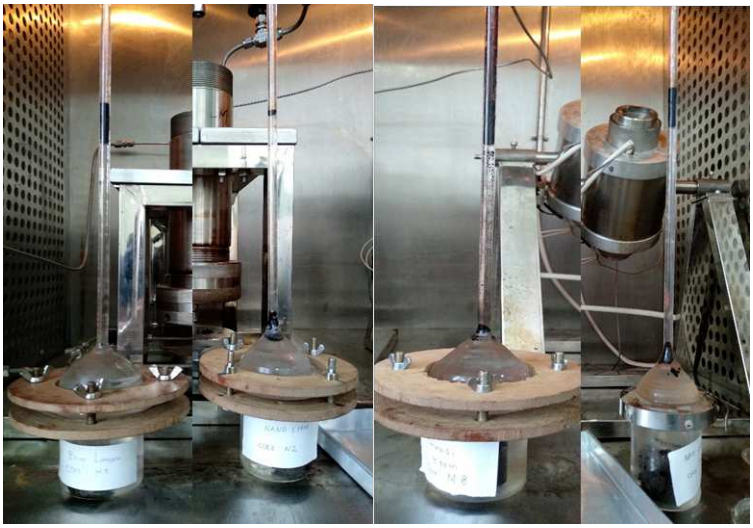

Figure 3. The imbibition process, Day 2.

Figure 4. The imbibition process, Day 3.

Figure 5. The imbibition process, Day 4.

Figure 6. The imbibition process, Day 5.

Figure 7. The imbibition process, Day 6.

Figure 8. Core condition at first day of imbibition process

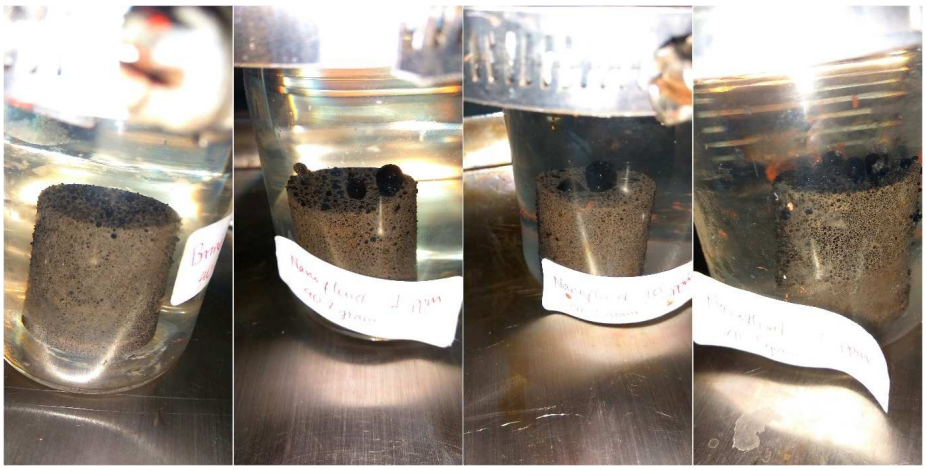

Figure 9. Core condition at sixth day of imbibition process

B. Numerical simulation flowchart

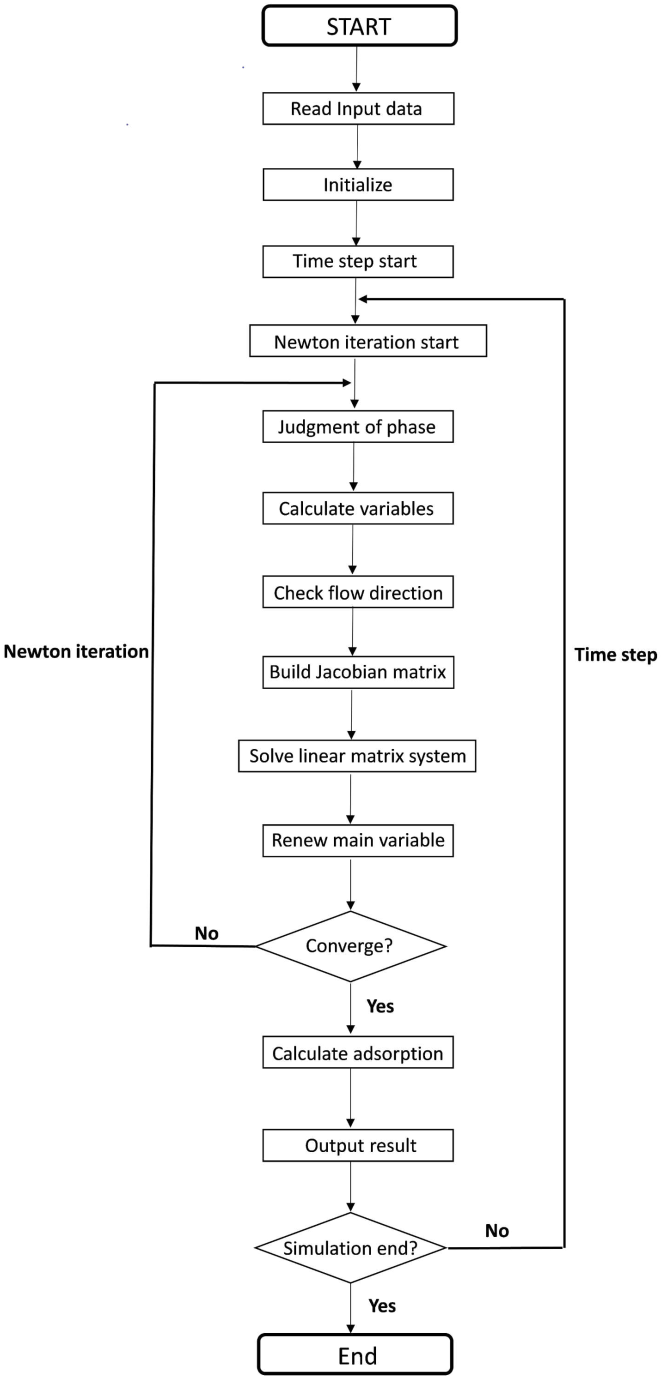

List of research achievements for application of Doctor of Engineering, Waseda University

Full Name : WIJAYANTO Tito seal or signature

Date Submitted(yyyy/mm/dd): 2021/12/16

種類別 (By Type)	題名、 発表・発行掲載誌名、 発表・発行年月、 連名者（申請者含む） (theme, journal name, date & year of publication, name of authors inc. yourself)
○ *Peer-reviewed journal*	Wijayanto, T., Kurihara, M., Kurniawan, T., and Muraza, O. (July 2019). Experimental Investigation of Aluminosilicate NPs for Enhanced Recovery of Waxy Crude Oil. *Energy & Fuels* , 33(7), pp.6076-6082.
○ *Peer-reviewed journal*	Wijayanto, T., Iskandar, U.P., Kurihara, M., Muraza, O., and Marhaendrajana, T. (2021). Application of functionalized cationic-acidic silica-alumina-based nanofluids for enhanced oil recovery. *Journal of the Japanese Association for Petroleum Technology* , 86(3), pp.194-204.
○ *Peer-reviewed journal*	Yahya, Z.N.M., Puspaseruni, N.P., Kurnia, R., Wahyuningrum, D., Mulyani, I., Wijayanto, T., Kurihara, M., Waskito, S.S., Aslam, B.M. and Marhaendrajana, T. (2022). The effect of aluminosilicate in anionic–nonionic surfactant mixture on wetness and interfacial tension in its application for enhanced oil recovery. *Energy Reports* , 8, pp.1013-1025.
Academic presentation	Experimental investigation for enhanced oil recovery using nano-solutions, 2019 JOGMEC-Joint Research Report Meeting, March 2020.
Academic presentation	Experimental investigation for enhanced oil recovery using nano-solutions, 2019 JAPEX Research Report Meeting, March 2020.
Academic presentation	Silica-alumina nanoparticles for enhanced oil recovery, EOR knowledge-sharing forum, Petroleum Engineering Department Institute Technology of Bandung, January 2017.
Academic presentation	Silica-alumina nanoparticles for enhanced oil recovery, EOR knowledge-sharing forum, Lemigas Research and Development Centre for Oil and Gas Technology., July 2016.